

HIGGS BOSONS: THEORY AND SEARCHES

Updated May 2010 by G. Bernardi (LPNHE, CNRS/IN2P3, U. of Paris VI & VII), M. Carena (Fermi National Accelerator Laboratory and the University of Chicago), and T. Junk (Fermi National Accelerator Laboratory).

I. Introduction

Understanding the mechanism that breaks electroweak symmetry and generates the masses of all known elementary particles is one of the most fundamental problems in particle physics. The Higgs mechanism [1] provides a general framework to explain the observed masses of the W^\pm and Z gauge bosons by means of charged and neutral Goldstone bosons that end up as the longitudinal components of the gauge bosons. These Goldstone bosons are generated by the underlying dynamics of electroweak symmetry breaking (EWSB). However, the fundamental dynamics of the electroweak symmetry breaking are unknown. There are two main classes of theories proposed in the literature, those with weakly coupled dynamics - such as in the Standard Model (SM) [2] - and those with strongly coupled dynamics.

In the SM, the electroweak interactions are described by a gauge field theory based on the $SU(2)_L \times U(1)_Y$ symmetry group. The Higgs mechanism posits a self-interacting complex doublet of scalar fields, and renormalizable interactions are arranged such that the neutral component of the scalar doublet acquires a vacuum expectation value $v \approx 246$ GeV, which sets the scale of EWSB. Three massless Goldstone bosons are generated, which are absorbed to give masses to the W^\pm and Z gauge bosons. The remaining component of the complex doublet becomes the Higgs boson - a new fundamental scalar particle. The masses of all fermions are also a consequence of EWSB since the Higgs doublet is postulated to couple to the fermions through Yukawa interactions. If the Higgs boson mass m_H is below ~ 180 GeV, all fields remain weakly interacting up to the Planck scale, M_{Pl} .

The validity of the SM as an effective theory describing physics up to the Planck scale is questionable, however, because

of the following “naturalness” argument. All fermion masses and dimensionless couplings are logarithmically sensitive to the scale Λ at which new physics becomes relevant. In contrast, scalar squared masses are quadratically sensitive to Λ . Thus, the observable SM Higgs mass has the following form:

$$m_H^2 = (m_H^2)_0 + \frac{kg^2\Lambda^2}{16\pi^2},$$

where $(m_H)_0$ is a fundamental parameter of the theory. The second term is a one-loop correction in which g is an electroweak coupling and k is a constant, presumably of $\mathcal{O}(1)$, that is calculable within the low-energy effective theory. The two contributions arise from independent sources and one would not expect that the observable Higgs boson mass is significantly smaller than either of the two terms. Hence, if the scale of new physics Λ is much larger than the electroweak scale, unnatural cancellations must occur to remove the quadratic dependence of the Higgs boson mass on this large energy scale and to give a Higgs boson mass of order of the electroweak scale, as required from unitarity constraints [3,4], and as preferred by precision measurements of electroweak observables [5]. Thus, the SM is expected to be embedded in a more fundamental theory which will stabilize the hierarchy between the electroweak scale and the Planck scale in a natural way. A theory of that type would usually predict the onset of new physics at scales of the order of, or just above, the electroweak scale. Theorists strive to construct models of new physics that keep the successful features of the SM while curing its shortcomings, including the absence of a dark matter candidate or an electroweak scale explanation of the observed baryon asymmetry of the universe.

In the weakly-coupled approach to electroweak symmetry breaking, supersymmetric (SUSY) extensions of the SM provide a possible explanation for the stability of the electroweak energy scale in the presence of quantum corrections [7]. These theories predict a spectrum of Higgs scalars [8]. The properties of the lightest Higgs scalar often resemble those of the SM Higgs boson, with a mass that is predicted to be less than 135 GeV [9] in the simplest supersymmetric model. Additional neutral and charged Higgs bosons with masses of order of the weak scale

are also predicted. Moreover, low-energy supersymmetry with a supersymmetry breaking scale of order 1 TeV allows for grand unification of the electromagnetic, weak and strong gauge interactions in a consistent way, strongly supported by the prediction of the electroweak mixing angle at low energy scales, with an accuracy at the percent level [10,11].

Alternatively, new strong interactions near the TeV scale can induce strong breaking of the electroweak symmetry [12]. Recently, so-called “Little Higgs” models have been proposed in which the scale of the new strong interactions is pushed up above 10 TeV [13], and the lightest Higgs scalar resembles the weakly-coupled SM Higgs boson.

Alternatively, a new approach to electroweak symmetry breaking has been explored in which extra space dimensions beyond the usual $3 + 1$ dimensional space-time are introduced [14] with characteristic sizes of order $(1 \text{ TeV})^{-1}$. In such scenarios, the mechanisms for electroweak symmetry breaking are inherently extra-dimensional and the resulting Higgs phenomenology can depart significantly from the SM paradigm [15].

Prior to 1989, when the e^+e^- collider LEP at CERN came into operation, searches for Higgs bosons were sensitive only to Higgs bosons with masses of a few GeV and below [16]. In the LEP1 phase, the collider operated at center-of-mass energies close to M_Z . During the LEP2 phase, the energy was increased in steps, reaching 209 GeV in the year 2000 before the final shutdown. The combined data of the four LEP experiments, ALEPH, DELPHI, L3, and OPAL, was sensitive to neutral Higgs bosons with masses up to about 115 GeV and to charged Higgs bosons with masses up to about 90 GeV [17,18].

The search for the Higgs boson continues at the Tevatron $p\bar{p}$ collider, operating at a center-of-mass energy of 1.96 TeV. The sensitivity of the two experiments, CDF and DØ, is improving, and with the integrated luminosity collected so far, is already high enough to probe SM Higgs boson masses beyond the LEP reach [19]. Other neutral and charged Higgs particles postulated in most theories beyond the SM are also actively sought at the Tevatron. The searches for Higgs bosons will continue with significantly higher sensitivities in the coming

years at the LHC pp collider and are expected to cover masses up to about 1 TeV for the SM Higgs boson [20,21]. Once evidence for the dynamics of electroweak symmetry breaking is obtained, a more complete understanding of the mechanism will require measurements at future e^+e^- [22] and perhaps $\mu^+\mu^-$ colliders [23].

In order to keep this review up to date, some unpublished results are quoted. LEP results are marked with (*) in the reference list and can be accessed conveniently from the public web page

lephiggs.web.cern.ch/LEPHIGGS/pdg2008/index.html.

Preliminary results from the CDF collaboration are marked with (**) and can be obtained from the public web page

<http://www-cdf.fnal.gov/physics/physics.html>;

those from D \emptyset are marked with (***) and can be obtained at
<http://www-d0.fnal.gov/Run2Physics/WWW/results.htm>.

II. The Standard Model Higgs Boson

In the SM, the Higgs boson mass is given by $m_H = \sqrt{\lambda/2} v$, where λ is the Higgs self-coupling parameter and v is the vacuum expectation value of the Higgs field, $v = (\sqrt{2}G_F)^{-1/2} \approx 246$ GeV, fixed by the Fermi coupling G_F , which is determined precisely from muon decay measurements [24]. Since λ is presently unknown, the value of the SM Higgs boson mass m_H cannot be predicted. However, besides the upper bound on the Higgs boson mass from unitarity constraints [3,4], additional theoretical arguments place approximate upper and lower bounds on m_H [25]. There is an upper bound based on the perturbativity of the theory up to the scale Λ at which the SM breaks down, and a lower bound derived from the stability of the Higgs potential. If m_H is too large, then the Higgs self-coupling diverges at some scale Λ below the Planck scale. If m_H is too small, then the Higgs potential develops a second (global) minimum at a large value of the scalar field of order Λ . New physics must enter at a scale Λ or below, so that the global minimum of the theory corresponds to the observed $SU(2)_L \times U(1)_Y$ broken vacuum with $v = 246$ GeV. Given a

value of Λ , one can compute the minimum and maximum allowed Higgs boson mass. Conversely, the value of m_H itself can provide an important constraint on the scale up to which the SM remains successful as an effective theory. In particular, a Higgs boson with mass in the range $130 \text{ GeV} \lesssim m_H \lesssim 180 \text{ GeV}$ is consistent with an effective SM description that survives all the way to the Planck scale, although the hierarchy problem between the electroweak scale and $\Lambda = M_{\text{Pl}}$ still persists. The lower bound on m_H can be reduced to about 115 GeV [26], if one allows for the electroweak vacuum to be metastable, with a lifetime greater than the age of the universe.

The SM Higgs couplings to fundamental fermions are proportional to the fermion masses, and the couplings to bosons are proportional to the squares of the boson masses. In particular, the SM Higgs boson is a CP -even scalar, and its couplings to gauge bosons, Higgs bosons and fermions are given by:

$$\begin{aligned} g_{Hf\bar{f}} &= \frac{m_f}{v}, & g_{HVV} &= \frac{2m_V^2}{v}, & g_{HHVV} &= \frac{2m_V^2}{v^2} \\ g_{HHH} &= \frac{3m_H^2}{v} & g_{HHHH} &= \frac{3m_H^2}{v^2} \end{aligned}$$

where $V = W^\pm$ or Z . In Higgs boson production and decay processes, the dominant mechanisms involve the coupling of the H to the W^\pm , Z and/or the third generation quarks and leptons. The Higgs boson's coupling to gluons, Hgg , is induced at leading order by a one-loop graph in which the H couples to a virtual $t\bar{t}$ pair. Likewise, the Higgs boson's coupling to photons, $H\gamma\gamma$, is also generated via loops, although in this case the one-loop graph with a virtual W^+W^- pair provides the dominant contribution [8]. Reviews of the SM Higgs boson's properties and its phenomenology, with an emphasis on the impact of loop corrections to the Higgs boson decay rates and cross sections, can be found in Refs. [27,28].

The cross sections for the production of SM Higgs bosons are summarized in Fig. 1 for $p\bar{p}$ collisions at the Tevatron, and in Fig. 2 for pp collisions at the LHC [29]. The cross section for the $gg \rightarrow H + X$ process is known at next-to-next-to-leading order (NNLO) in QCD, in the large top-mass limit, and at NLO in QCD for arbitrary top mass [30]. The NLO QCD

corrections approximately double the leading-order prediction, and the NNLO corrections add approximately 50% to the NLO prediction. NLO electroweak corrections (not included in the figures) range between 0 and 6% of the LO term [31]. Mixed QCD-electroweak corrections $O(\alpha\alpha_s)$ are computed in [32]. In addition, soft-gluon contributions to the cross sections have been resummed at next-to-next-to-leading logarithmic (NNLL) and NNNLL accuracy [33]. Updated predictions for the gluon fusion cross sections using the most recent parametrizations of parton distribution functions at next-to-next-to-leading order can be found in [32,34]. An additional enhancement of the cross section is obtained when a resummation of the kinematically enhanced terms in the time-like gluon form factor is performed [35]. At LHC and Tevatron energies, and for intermediate Higgs-boson masses, this increases the cross section by about 6% compared with that obtained using soft-gluon resummation alone, and by about 10% compared with the fixed-order results at NNLO. Certain search strategies look for Higgs boson production in association with jets. In the heavy top quark mass limit, Higgs boson production cross section in association with one jet is considered in Refs. [36–39] and in association with two jets in Refs. [40,41].

The cross sections for the associated production processes $q\bar{q} \rightarrow W^\pm H + X$ and $q\bar{q} \rightarrow ZH + X$ are known at NNLO for the QCD corrections and at NLO for the electroweak corrections [42,43]. The residual uncertainty is rather small, less than 5%. For the vector boson fusion processes $qq \rightarrow qqH + X$, corrections to the production cross section are known at NNLO in QCD and the remaining theoretical uncertainties are approximately 2% [44]. The cross section for the associated production process $t\bar{t}H$ has been calculated at NLO in QCD [45], while the bottom fusion Higgs boson production cross section is known at NNLO in the case of five quark flavors [42,46,47].

The branching ratios for the most relevant decay modes of the SM Higgs boson are shown in Fig. 3 as functions of m_H , and the total decay width is shown in Fig. 4, also as function of m_H [28,48]. For masses below 135 GeV, decays to fermion pairs dominate, of which the decay $H \rightarrow b\bar{b}$ has the largest branching

ratio. Decays to $\tau^+\tau^-$, $c\bar{c}$ and gluon pairs together contribute less than 15%. For such low masses, the total decay width is less than 10 MeV. For Higgs boson masses above 135 GeV, the W^+W^- decay dominates (below the W^+W^- threshold, one of the W bosons is virtual) with an important contribution from $H \rightarrow ZZ$, and the decay width rises rapidly, reaching about 1 GeV at $m_H = 200$ GeV and 100 GeV at $m_H = 500$ GeV. Above the $t\bar{t}$ threshold, the branching ratio into top-quark pairs increases rapidly as a function of the Higgs boson mass, reaching a maximum of about 20% at $m_H \sim 450$ GeV.

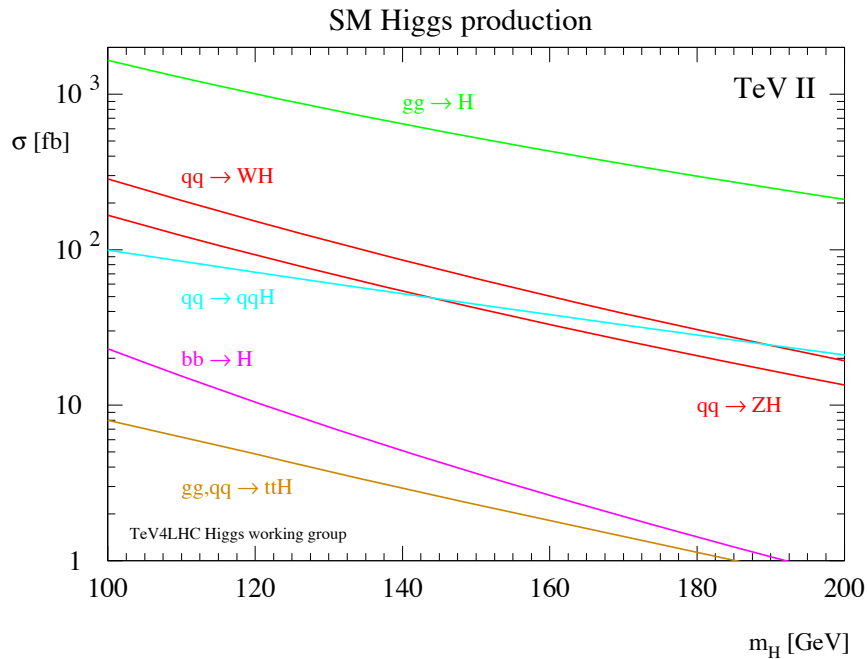


Figure 1: SM Higgs boson production cross sections for $p\bar{p}$ collisions at 1.96 TeV, from Ref. 29 and references therein. Color version at end of book.

Searches for the SM Higgs Boson at LEP

The principal mechanism for producing the SM Higgs boson in e^+e^- collisions at LEP energies is Higgs-strahlung in the s -channel, $e^+e^- \rightarrow HZ$ [49]. The Z boson in the final state is either virtual (LEP1), or on mass shell (LEP2). The SM Higgs

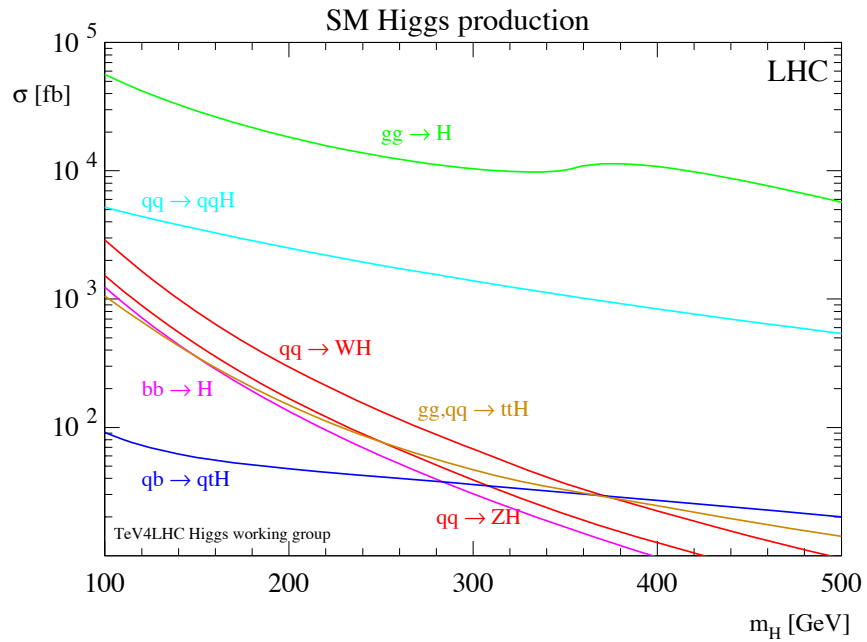


Figure 2: SM Higgs boson production cross sections for pp collisions at 14 TeV [29]. Color version at end of book.

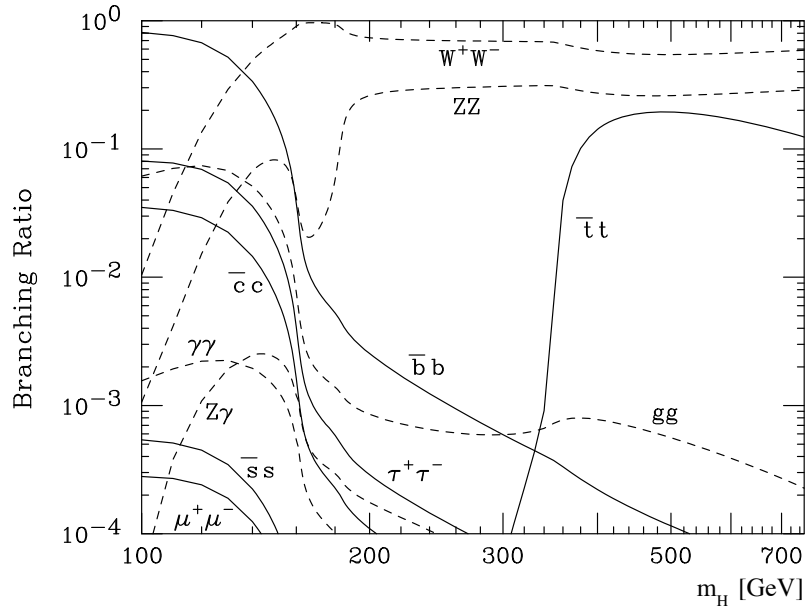


Figure 3: Branching ratios for the main decays of the SM Higgs boson [28,48].

boson can also be produced by W^+W^- and ZZ fusion in the t -channel [50], but at LEP these processes have small cross

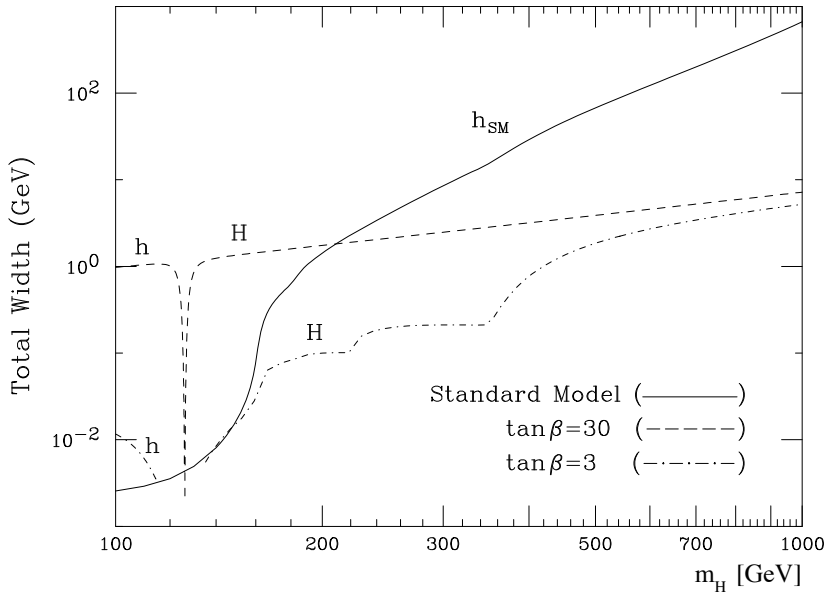


Figure 4: The total decay width of the SM Higgs boson, shown as a function of m_H [48]. Also shown are the decay widths for the CP-even neutral Higgs bosons, h and H , for two choices of $\tan\beta$, in the MSSM benchmark scenario m_h -max, described in Section III.

sections. The sensitivity of the LEP searches to the Higgs boson is primarily a function of the center-of-mass energy, E_{CM} . For $m_H < E_{\text{CM}} - M_Z$, the cross section is quite large, of order 1 pb or more, while for $m_H > E_{\text{CM}} - M_Z$, the cross section is smaller by an order of magnitude or more.

During the LEP1 phase, the ALEPH, DELPHI, L3 and OPAL collaborations analyzed over 17 million Z decays and set lower bounds of approximately 65 GeV on the mass of the SM Higgs boson [51]. At LEP2, substantial data samples were collected at center-of-mass energies up to 209 GeV.

Each production and decay mode was analyzed separately. Data recorded at each center-of-mass energy were studied independently and the results from the four LEP experiments were then combined. Distributions of neural network discriminants which are functions of reconstructed event quantities such as invariant masses and b -tagging discriminants were assembled for the data, and also for the signal and background predictions. The CL_s method [52] was used to compute the observed

and expected limits on the Higgs boson production cross section as functions of the Higgs boson mass sought, and from that, a lower bound on m_H was derived. The p -value for the background-only hypothesis, which is the probability for the background model to produce a fluctuation as signal-like as that seen in the data or more, was also computed.

Higgs bosons were sought in four final state topologies: The four-jet topology in which $H \rightarrow b\bar{b}$ and $Z \rightarrow q\bar{q}$; the final states with tau leptons produced in the processes $H \rightarrow \tau^+\tau^-$ where $Z \rightarrow q\bar{q}$, together with the mode $H \rightarrow b\bar{b}$ with $Z \rightarrow \tau^+\tau^-$; the missing energy topology produced mainly in the process $H \rightarrow b\bar{b}$ with $Z \rightarrow \nu\bar{\nu}$, and finally the leptonic states $H \rightarrow b\bar{b}$ with $Z \rightarrow e^+e^-, \mu^+\mu^-$. At LEP1, only the modes with $Z \rightarrow \ell^+\ell^-$ and $Z \rightarrow \nu\bar{\nu}$ were used because the backgrounds in the other channels were prohibitive. For the data collected at LEP2, all decay modes were used.

For very light Higgs bosons, with $m_H < 2m_\tau$, the decay modes exploited above are not kinematically allowed, and decays to jets, muon pairs, pion pairs, and lighter particles dominate, depending sensitively on m_H . For very low masses, OPAL’s decay-mode independent search [53] for the Bjorken process $e^+e^- \rightarrow S^0Z$, where S^0 denotes a generic neutral, scalar particle, provides sensitivity. This search is based on studies of the recoil mass spectrum in events with $Z \rightarrow e^+e^-$ and $Z \rightarrow \mu^+\mu^-$ decays, and on the final states $Z \rightarrow \nu\bar{\nu}$ and $S^0 \rightarrow e^+e^-$ or photons. Upper bounds on the cross section are produced for scalar masses between 1 KeV and 100 GeV.

The LEP searches did not show any conclusive evidence for the production of a SM Higgs boson. However, in the LEP2 data, ALEPH reported an excess of about three standard deviations, suggesting the production of a SM Higgs boson with mass ~ 115 GeV [54]. Analyses of the data from DELPHI [55], L3 [56], and OPAL [57] did not show evidence for such an excess, but could not, however, exclude a 115 GeV Higgs boson at the 95% C.L. When the data of the four experiments were combined, the overall significance of a possible signal at $m_H = 115$ GeV was low, as given by the background-only p -value of 0.09 [17]. The same combination of the LEP data

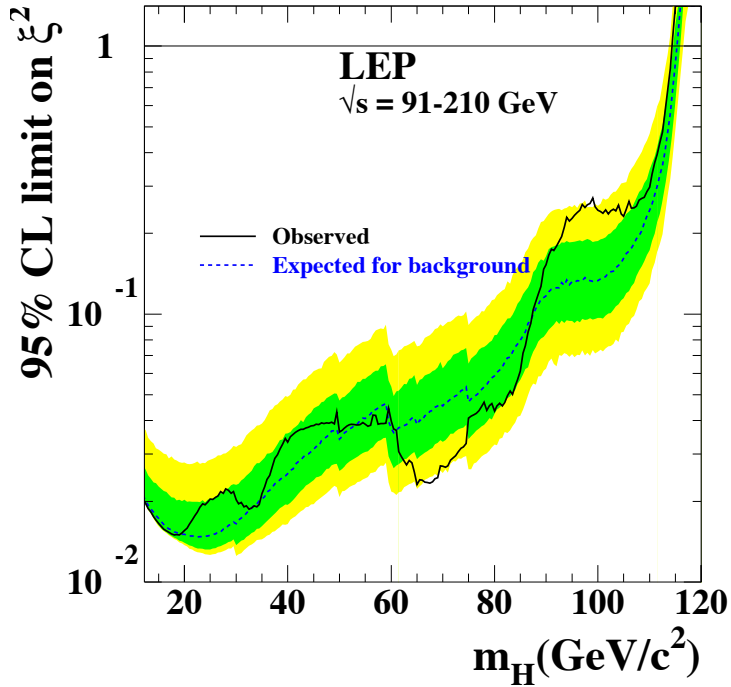


Figure 5: The 95% confidence level upper bound on the ratio $\xi^2 = (g_{HZZ}/g_{HZZ}^{\text{SM}})^2$ [17]. The solid line indicates the observed limit, and the dashed line indicates the median limit expected in the absence of a Higgs boson signal. The dark and light shaded bands around the expected limit line correspond to the 68% and 95% probability bands, indicating the range of statistical fluctuations of the expected outcomes. The horizontal line corresponds to the Standard Model coupling. Standard Model Higgs boson decay branching fractions are assumed. Color version at end of book.

yields a 95% C.L. lower bound of 114.4 GeV for the mass of the SM Higgs boson. The median limit one would expect to obtain in a large ensemble of identical experiments with no signal present is 115.3 GeV. Fig. 5 shows the observed production cross section limits, relative to the SM Higgs boson production rate (including vector-boson fusion), assuming SM Higgs boson branching ratios.

Indirect Constraints on the SM Higgs Boson

Indirect experimental bounds for the SM Higgs boson mass are obtained from fits to precision measurements of electroweak observables. The Higgs boson contributes to the W^\pm and Z vacuum polarization through loop effects, leading to a logarithmic sensitivity of the ratio of the W^\pm and Z gauge boson masses on the Higgs boson mass. A global fit to precision electroweak data, accumulated in the last two decades at LEP, SLC, the Tevatron, and elsewhere, gives $m_H = 87^{+35}_{-26}$ GeV, or $m_H < 157$ GeV at 95% C.L. [5]. The top quark contributes to the W^\pm boson vacuum polarization through loop effects that depend quadratically on the top mass, which plays an important role in the global fit. A top quark mass of 173.1 ± 1.3 GeV [58] and a W^\pm boson mass of 80.399 ± 0.023 GeV [59] were used. If the direct LEP search limit of $m_H > 114.4$ GeV is taken into account, an upper limit of $m_H < 186$ GeV at 95% C.L. is obtained.

Searches for the SM Higgs Boson at the Tevatron

At the Tevatron, the most important SM Higgs boson production processes are gluon fusion ($gg \rightarrow H$) and Higgs boson production in association with a vector boson ($W^\pm H$ or ZH) [60]. For masses less than about 135 GeV, the most promising discovery channels are $W^\pm H$ and ZH with $H \rightarrow b\bar{b}$. The contribution of $H \rightarrow W^*W$ is dominant at higher masses, $m_H > 135$ GeV. Using this decay mode, both the direct ($gg \rightarrow H$) and the associated production ($p\bar{p} \rightarrow W^\pm H$ or ZH) channels are explored, and the results of both Tevatron experiments are combined to maximize the sensitivity to the Higgs boson.

The signal-to-background ratio is much smaller in the Tevatron searches than in the LEP analyses, and the systematic uncertainties on the estimated background rates are typically larger than the signal rates. In order to estimate the background rates in the selected samples more accurately, auxiliary measurements are made in data samples which are expected to be depleted in Higgs boson signal. These auxiliary samples are chosen to maximize the sensitivity to each specific background in turn. Then, Monte Carlo simulations are used to

extrapolate these measurements into the Higgs signal regions. The dominant physics backgrounds such as top-pair, diboson, $W^\pm b\bar{b}$, and single top production are estimated by Monte Carlo simulations in this way, i.e., after having been tuned or verified by corresponding measurements in dedicated analyses, thereby reducing the uncertainty on the total background estimate. The uncertainties on the background rates diminish with increasing integrated luminosity because increasingly larger data samples are used to constrain them, and thus these uncertainties are not expected to be limiting factors in the sensitivity of the searches.

At Higgs boson masses of 150 GeV and below, the searches for associated production, $p\bar{p} \rightarrow W^\pm H, ZH$, are performed in different channels:

- a) $p\bar{p} \rightarrow W^\pm H$, where the W^\pm decays leptonically and $H \rightarrow b\bar{b}$. These searches have been published by CDF using 2.7 fb^{-1} of data [61] and by DØ using 1.1 fb^{-1} of data [62]. The latest updates as of this review are based on 4.8 fb^{-1} of data from CDF [63] and 5.0 fb^{-1} from DØ [64]; the Higgs boson production cross section limits obtained by both collaborations are four to five times higher than the SM expectation in this channel for a Higgs boson mass of 115 GeV. These updates use advanced analysis techniques such as neural networks to separate a potential signal from the background processes, and also to separate correctly identified b -jets from jets originating from gluons or from u, d, s or c quarks, mistakenly identified as b -jets.
- b) $p\bar{p} \rightarrow ZH$, where the Z decays into $\nu\bar{\nu}$, is also a sensitive channel, but, since the final state is characterized by missing transverse energy and two b -jets, multijet backgrounds without Z bosons require special care. The sensitivity of this search is enhanced by $W^\pm H$ events in which the charged lepton from the W^\pm decay escapes detection; these events have the same experimental signature as the $ZH \rightarrow \nu\bar{\nu}$ signal. The CDF Collaboration has published a result in this channel using 2.1 fb^{-1} of data [65] and the DØ Collaboration has published a result in this channel with 5.2 fb^{-1} of data [66] with optimized triggers and selection criteria which improve the signal acceptance, as well as refined analysis techniques. An

update with 3.6 fb^{-1} (CDF [67]) was also released in 2009. The sensitivity of these channels is comparable to that obtained in the $W^\pm H$ channel.

- c) $p\bar{p} \rightarrow ZH$, where the Z decays into charged leptons (e or μ), suffers from a smaller Z branching fraction, but it has a lower background rate. Both collaborations constrain the kinematics of the events to improve the reconstructed mass resolution. The sensitivity of these channels is not much lower than that of the previous two channels. The CDF Collaboration has published a result in this channel using 2.7 fb^{-1} of data [68] and the DØ Collaboration has published a result based on 0.45 fb^{-1} of data [69]. Preliminary updates with 4.2 fb^{-1} of data are available from both CDF and DØ [70,71].
- d) Both Tevatron collaborations search for SM $H \rightarrow \tau^+\tau^-$, where the $gg \rightarrow H$, WH , ZH , and vector-boson fusion production processes are considered [72,73]. The DØ publication has been updated with a 4.9 fb^{-1} data sample [74]. DØ also includes a search for $WH \rightarrow \tau\nu b\bar{b}$, using a 4.0 fb^{-1} data sample [75]. This final state is partly covered by CDF in its isolated-track selection [76], in a 4.3 fb^{-1} data sample. These analyses benefit from the more inclusive production mechanisms considered, but the $H \rightarrow \tau^+\tau^-$ decay branching fraction is significantly less than that to $b\bar{b}$, as shown in Fig. 3.
- e) Both Tevatron collaborations search for the SM process $H \rightarrow \gamma\gamma$, making use of all production modes. Since $\text{BR}(H \rightarrow \gamma\gamma)$ is so small in the SM, they contribute little to the SM combined sensitivity. Nonetheless, they set strong constraints on extended models, and thus are discussed later in this review.
- e) The CDF Collaboration has published a search in 2.0 fb^{-1} of data for $WH + ZH \rightarrow jj b\bar{b}$ [77], making use of signal events in which the vector boson decays to jets. While the expected signal yields are higher than in other modes due to the favorable branching fractions, the multijet backgrounds are also quite large.

When combining the low-mass channels of the two collaborations, the expected (observed) limit is 1.8 (2.7) times higher than the expected SM production cross section for

$m_H = 115$ GeV, as can be seen in Fig. 6 [78]. With the projected improvements in analysis sensitivity, and the accumulation of more integrated luminosity (12 fb^{-1} of data are expected by the end of 2011), the low-mass Higgs boson is expected to be probed at the Tevatron.

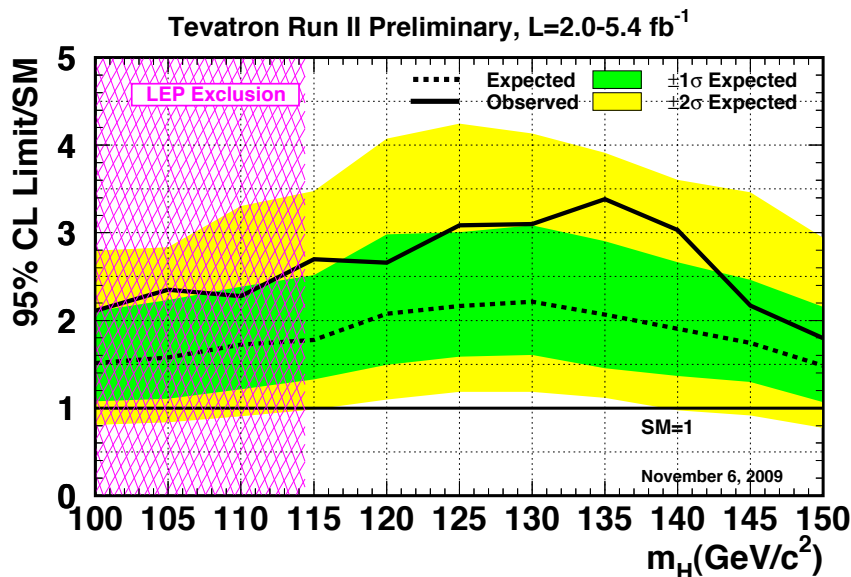


Figure 6: Upper bound on the SM Higgs boson cross section obtained by combining CDF and D \emptyset search results, as a function of the mass of the Higgs boson sought [78]. The limits are shown as a multiple of the SM cross section. The ratios of the different production and decay modes are assumed to be as predicted by the SM. The solid curve is the observed upper bound, and the dashed black curve is the median expected upper bound assuming no signal is present. The shaded bands show the 68% and 95% probability bands around the expected upper bound. Color version at end of book.

Around $m_H = 135$ GeV, where all branching fractions are below 50%, no channel is strongly dominant and the overall sensitivity is weaker. At these masses, the $WH \rightarrow$

WWW^* channel ¹ brings further sensitivity [79,80,81] beyond the $b\bar{b}$ channel alone.

To probe masses above 135 GeV, the dominant $H \rightarrow WW^*$ decay mode is best exploited. The dominant production mode is $gg \rightarrow H$ which can be used in this channel since the leptonic W boson decays distinguish the signal from backgrounds containing jets. Nonetheless, WH production, ZH production, and vector-boson fusion qqH production contribute additional signal in this channel which is used in the searches. The WW pair issued from a Higgs boson decay has a spin correlation which is different from that of the dominant background, electroweak WW production. These spin correlations are transmitted to the distributions of observed leptons, providing a handle to separate the signal from the background. The invariant mass of the Higgs boson decay products cannot be reconstructed due to the undetected neutrinos, but the sensitivity is nevertheless significant. Results were published with 4.8 fb^{-1} by CDF [82] and 5.4 fb^{-1} by DØ [83], together with the combination of these results [19], which are reproduced in Fig. 7. An expected (observed) upper limit is set on the $gg \rightarrow H$ cross section 0.9 (0.9) times the SM prediction at $m_H = 165 \text{ GeV}$ [78], a SM Higgs boson with mass between 162 and 166 GeV is excluded at the 95% C.L.

Overall, the combined CDF and DØ analyses are expected to test, at the 95% C.L. or better, the SM Higgs boson predictions for masses between the LEP limit and about 185 GeV before the end of Run II. The channels used at the Tevatron for Higgs boson masses below 130 GeV are different from those dominantly used at the LHC, hence with the full Run II luminosity, they are expected to provide complementary information if a low mass Higgs boson exists.

The SM Higgs boson production processes and branching ratios presented above are limited to the case of three generations of quarks and leptons. The existence of a fourth generation of fermions is compatible with present experimental bounds and

¹ The star indicates that below the $H \rightarrow W^+W^-$ threshold, one of the W^\pm bosons is virtual.

would have direct consequences on the SM Higgs boson production and decay branching ratios, and hence on Higgs searches at LEP, the Tevatron, and the LHC [84,85]. Current experimental searches bound the fourth generation quark masses to be above the top quark mass [86]. These additional heavy quarks lead to new contributions in the loop-induced couplings of the Higgs boson to gluons and photons, leading to a strong enhancement of the gluon fusion production rate and of the branching ratio of the Higgs boson decay into a pair of gluons. The branching ratios of Higgs boson decay to $b\bar{b}$, tau pairs, and pairs of W and Z bosons are reduced, although near $m_H \sim 2M_W$, the decay to a pair of W bosons still nearly saturates the decay width, even with the enhanced gluon decay. Due to a cancellation between the W and heavy fermion contributions, the photon decay channels may be further suppressed. The enhancement of the gluon fusion production rate makes the search channels using Higgs boson decays into tau leptons and W and Z bosons promising for a light Higgs boson. In addition, in the case of a fourth generation Majorana neutrino, exotic signals such as Higgs boson decay into same-sign dileptons may be possible.

The CDF and DØ search results in the $H \rightarrow W^+W^-$ decay mode have been used to test an extension of the SM with four generations of quarks and leptons, using only the $gg \rightarrow H \rightarrow W^+W^-$ mechanism [87]. The production cross section is computed at NNLO [88], and the decay branching fractions are computed using a modified version of HDECAY [28,84]. The excluded ratio to the fourth-generation prediction is shown in Fig. 8, excluding such a Higgs boson with a mass between 131 and 204 GeV. These limits limits are robust against other choices of the heavy fermion masses.

Studies to assess the sensitivity to diffractive Higgs boson production at the Tevatron and the LHC are being pursued [89]. Three different diffractive production mechanisms can be considered: exclusive production, $p\bar{p}, pp \rightarrow p + H + \bar{p}, p$; inclusive production, $p\bar{p}, pp \rightarrow X + H + Y$; and central inelastic production, $p\bar{p}, pp \rightarrow p + (HX) + \bar{p}, p$, where a plus sign indicates the presence of a rapidity gap. Tests of the different production mechanisms using appropriate final states in the Tevatron data

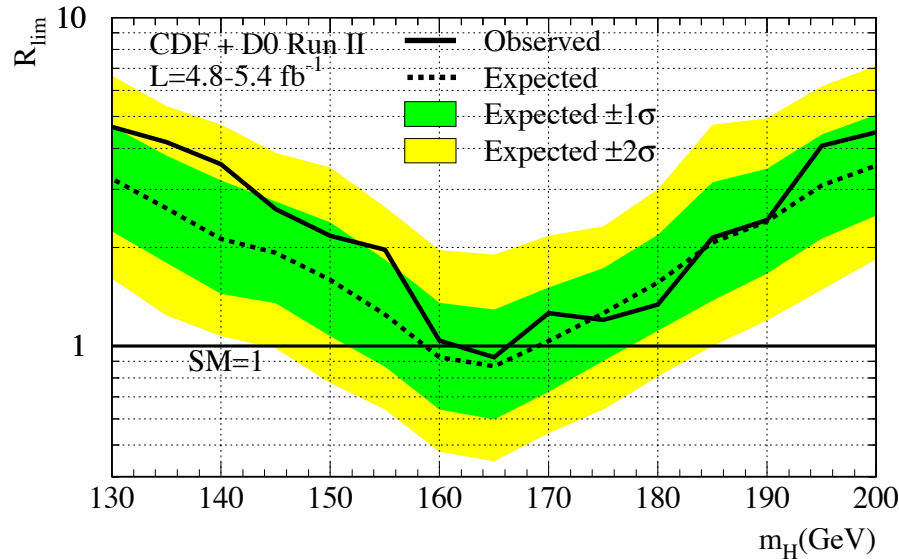


Figure 7: Upper bound on the SM Higgs boson cross section obtained by combining CDF and D \emptyset search results in the $H \rightarrow W^+W^-$ decay mode, as a function of the mass of the Higgs boson sought [19]. The limits are shown as a multiple of the SM cross section. The ratios of the different production and decay modes are assumed to be as predicted by the SM. The solid curve shows the observed upper bound, the dashed black curve shows the median expected upper bound assuming no signal is present. The shaded bands show the 68% and 95% probability bands around the expected upper bound. Color version at end of book.

are important for improving predictions for diffractive Higgs boson production at the LHC.

Prospects for SM Higgs Boson Searches at the LHC

At the LHC, the main production processes are gluon fusion ($gg \rightarrow H$), Higgs boson production in association with a vector boson ($W^\pm H$ or ZH) or with a top-quark pair ($t\bar{t}H$), and the vector boson fusion process (qqH or $q\bar{q}H$) [60]. This array of production and decay modes, together with a large integrated luminosity, allows for a variety of search channels. Search strategies have been explored in many analyses over the last years [20,21]. The searches in the inclusive channels

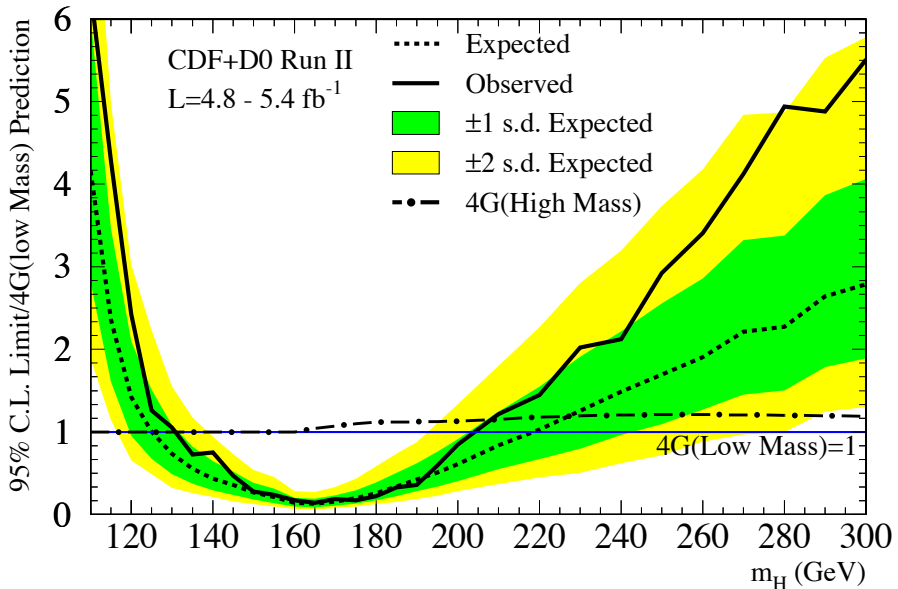


Figure 8: Upper bound on the Higgs boson cross section of the 4th generation sequential model obtained by combining CDF and DØ search results in the $H \rightarrow W^+W^-$ decay mode, as a function of the mass of the Higgs boson sought [87]. The limits are shown as a multiple of the cross section obtained in this extended model. The solid curve shows the observed upper bound, the dashed black curve shows the median expected upper bound assuming no signal is present, and the colored bands show the 68% and 95% probability bands around the expected upper bound. Color version at end of book.

$H \rightarrow \gamma\gamma$ (for low mass) and $H \rightarrow ZZ^* \rightarrow 4\ell$ (for high mass) will be complemented with more exclusive searches in order to strengthen the discovery potential, particularly at low mass. Vector boson fusion processes, making use of forward jet tagging and the decay modes $H \rightarrow \tau^+\tau^-$, $H \rightarrow \gamma\gamma$ as well as $H \rightarrow W^+W^-$ [90] will provide additional sensitivity. Other analyses, expected to be relevant at higher integrated luminosities, select Higgs boson decays to $b\bar{b}$ or $\gamma\gamma$ in association with a lepton from the decay of an associated W^\pm boson, Z boson, or top quark.

The projections of the ATLAS and CMS collaborations show that, with an integrated luminosity of $10 - 30 \text{ fb}^{-1}$ at a center-of-mass energy of 14 TeV, the SM Higgs boson is expected to be discovered if it exists and has a mass below 1 TeV. With a lower integrated luminosity, the discovery of a Higgs boson with a mass below 130 GeV is challenging. If the Higgs boson’s mass is in this range, a few years of running may be needed to discover it. However, the combination of the results in all channels of the two experiments could allow for a 5σ discovery with about 5 fb^{-1} of data, once the detectors and the composition of the selected event samples are understood [91,92].

If a SM Higgs boson is discovered, its properties could be studied at the LHC. Its mass could be measured by each experiment with a precision of $\sim 0.1\%$ in the 100–400 GeV mass range [21,93]. This projection is based on the invariant mass reconstruction from electromagnetic calorimeter objects, using the decays $H \rightarrow \gamma\gamma$ or $H \rightarrow ZZ^* \rightarrow 4\ell$. The precision would be degraded at higher masses because of the larger decay width, but even at $m_H \sim 700 \text{ GeV}$ a precision of 1% on m_H is expected to be achievable. The width of the SM Higgs boson would be too narrow to be measured directly for $m_H < 200 \text{ GeV}$; nonetheless, it could be constrained indirectly using partial width measurements [94,95]. For $300 < m_H < 700 \text{ GeV}$, a direct measurement of the decay width could be performed with a precision of about 6%. The possibilities for measuring other properties of the Higgs boson, such as its spin, its CP -eigenvalue, its couplings to bosons and fermions, and its self-coupling, have been investigated in numerous studies [21,93,96–98]. Given a sufficiently high integrated luminosity (300 fb^{-1}), most of these properties are expected to be accessible to analysis for some specific mass ranges. The measurement of Higgs self-couplings, however, appears to be impossible at the LHC, although a luminosity upgrade, the so-called Super-LHC, could allow for such a measurement. The results of these measurements could either firmly establish the Higgs mechanism, or point the way to new physics.

III. Higgs Bosons in the MSSM

Electroweak symmetry breaking driven by a weakly-coupled elementary scalar sector requires a mechanism to explain the smallness of the electroweak symmetry breaking scale compared with the Planck scale [99]. Within supersymmetric extensions of the SM, supersymmetry-breaking effects, whose origins may lie at energy scales much larger than 1 TeV, can induce a radiative breaking of the electroweak symmetry due to the effects of the large Higgs-top quark Yukawa coupling [100]. In this way, the electroweak symmetry breaking scale is intimately tied to the mechanism of supersymmetry breaking. Thus, supersymmetry provides an explanation for the stability of the hierarchy of scales, provided that the supersymmetry-breaking masses are of $\mathcal{O}(1 \text{ TeV})$ or less [99].

A fundamental theory of supersymmetry breaking is unknown at this time. Nevertheless, one can parameterize the low-energy theory in terms of the most general set of soft supersymmetry-breaking renormalizable operators [101]. The Minimal Supersymmetric extension of the Standard Model (MSSM) [102] associates a supersymmetric partner to each gauge boson and chiral fermion of the SM, and provides a realistic model of physics at the weak scale. However, even in this minimal model with the most general set of soft supersymmetry-breaking terms, more than 100 new parameters are introduced [103]. Fortunately, only a small number of these parameters impact the Higgs phenomenology through tree level and quantum effects.

The MSSM contains the particle spectrum of a two-Higgs-doublet model (2HDM) extension of the SM and the corresponding supersymmetric partners. Two Higgs doublets, H_u and H_d , are required to ensure an anomaly-free SUSY extension of the SM and to generate mass for both “up”-type and “down”-type quarks and charged leptons [8]. After the spontaneous breaking of the electroweak symmetry, five physical Higgs particles are left in the spectrum: one charged Higgs pair, H^\pm , one CP -odd scalar, A , and two CP -even states, H and h .

The supersymmetric structure of the theory imposes constraints on the Higgs sector of the model. In particular, the

parameters of the Higgs self-interaction are given by the gauge coupling constants. As a result, all Higgs sector parameters at tree level are determined by only two free parameters: the ratio of the H_u and H_d vacuum expectation values,

$$\tan \beta = v_u/v_d,$$

with $v_u^2 + v_d^2 \approx (246 \text{ GeV})^2$; and one Higgs boson mass, conventionally chosen to be m_A . The other tree-level Higgs boson masses are then given in terms of these parameters

$$m_{H^\pm}^2 = m_A^2 + M_W^2$$

$$m_{H,h}^2 = \frac{1}{2} \left[m_A^2 + M_Z^2 \pm \sqrt{(m_A^2 + M_Z^2)^2 - 4(M_Z m_A \cos 2\beta)^2} \right]$$

and α is the angle that diagonalizes the CP -even Higgs squared-mass matrix.

An important consequence of these mass formulae is that the mass of the lightest CP -even Higgs boson is bounded from above:

$$m_h \leq M_Z |\cos 2\beta|.$$

This contrasts sharply with the SM, in which this Higgs boson mass is only constrained by perturbativity and unitarity bounds. In the large m_A limit, also called the decoupling limit [104], one finds $m_h^2 \simeq (M_Z \cos 2\beta)^2$ and $m_A \simeq m_H \simeq m_{H^\pm}$, up to corrections of $\mathcal{O}(M_Z^2/m_A)$. Below the scale m_A , the effective Higgs sector consists only of h , which behaves very similarly to the SM Higgs boson.

The phenomenology of the Higgs sector depends on the couplings of the Higgs bosons to gauge bosons, and fermions. The couplings of the two CP -even Higgs bosons to W^\pm and Z bosons are given in terms of the angles α and β by

$$g_{hVV} = g_V m_V \sin(\beta - \alpha) \quad g_{HVV} = g_V m_V \cos(\beta - \alpha),$$

where $g_V \equiv 2m_V/v$. There are no tree-level couplings of A or H^\pm to VV . The couplings of the Z boson to two neutral Higgs bosons, which must have opposite CP -quantum numbers, are given by

$$g_{hAZ} = g_Z \cos(\beta - \alpha)/2$$

$$g_{HAZ} = -g_Z \sin(\beta - \alpha)/2.$$

Charged Higgs-W boson couplings to neutral Higgs bosons and four-point couplings of vector bosons and Higgs bosons can be found in Ref. 8.

The tree-level Higgs couplings to fermions obey the following property: the neutral components of one Higgs doublet couples exclusively to down-type fermion pairs while the neutral components of the other couples exclusively to up-type fermion pairs [8,105]. This pattern of Higgs-fermion couplings defines the Type-II (2HDM)². Fermion masses are generated when the neutral Higgs components acquire vacuum expectation values. The relations between Yukawa couplings and fermion masses are (in third-generation notation)

$$\begin{aligned} h_b &= \sqrt{2} m_b/v_d = \sqrt{2} m_b/(v \cos \beta) \\ h_t &= \sqrt{2} m_t/v_u = \sqrt{2} m_t/(v \sin \beta). \end{aligned}$$

Similarly, one can define the Yukawa coupling of the Higgs boson to τ -leptons (the latter is a down-type fermion).

The couplings of the neutral Higgs bosons to $f\bar{f}$ relative to the SM value, $gm_f/2M_W$, are given by

$$\begin{aligned} h b\bar{b} : \quad -\sin \alpha / \cos \beta &= \sin(\beta - \alpha) - \tan \beta \cos(\beta - \alpha), \\ h t\bar{t} : \quad \cos \alpha / \sin \beta &= \sin(\beta - \alpha) + \cot \beta \cos(\beta - \alpha), \\ H b\bar{b} : \quad \cos \alpha / \cos \beta &= \cos(\beta - \alpha) + \tan \beta \sin(\beta - \alpha), \\ H t\bar{t} : \quad \sin \alpha / \sin \beta &= \cos(\beta - \alpha) - \cot \beta \sin(\beta - \alpha), \\ A b\bar{b} : \quad \gamma_5 \tan \beta, \quad A t\bar{t} : \quad \gamma_5 \cot \beta, \end{aligned}$$

where the γ_5 indicates a pseudoscalar coupling. In each relation above, the factor listed for $b\bar{b}$ also pertains to $\tau^+\tau^-$. The charged Higgs boson couplings to fermion pairs are given by

$$\begin{aligned} g_{H-t\bar{b}} &= \frac{g}{\sqrt{2}M_W} [m_t \cot \beta P_R + m_b \tan \beta P_L], \\ g_{H-\tau^+\nu} &= \frac{g}{\sqrt{2}M_W} [m_\tau \tan \beta P_L], \end{aligned}$$

² In the Type-I 2HDM, one field couples to all fermions while the other field is decoupled from them.

with $P_{L,R} = (1 \mp \gamma_5)/2$.

The Higgs couplings to down-type fermions can be significantly enhanced at large $\tan\beta$ in the following two cases: (*i*) If $m_A \gg M_Z$, then $|\cos(\beta - \alpha)| \ll 1$, $m_H \simeq m_A$, and the $b\bar{b}H$ and $b\bar{b}A$ couplings have equal strength and are significantly enhanced by a factor of $\tan\beta$ relative to the SM $b\bar{b}H$ coupling, whereas the VVH coupling is negligibly small. The values of the VVh and $b\bar{b}h$ couplings are equal to the corresponding couplings of the SM Higgs boson. (*ii*) If $m_A < M_Z$ and $\tan\beta \gg 1$, then $|\cos(\beta - \alpha)| \approx 1$ and $m_h \simeq m_A$. In this case, the $b\bar{b}h$ and $b\bar{b}A$ couplings have equal strength and are significantly enhanced by a factor of $\tan\beta$ relative to the SM $b\bar{b}H$ coupling, while the VVh coupling is negligibly small. In addition, the VVH coupling is equal in strength to the SM VVH coupling and one can refer to H as a SM-like Higgs boson, although the value of the $b\bar{b}H$ coupling can differ from the corresponding SM $b\bar{b}H$ coupling. Note that in both cases (*i*) and (*ii*) above, only two of the three neutral Higgs bosons have enhanced couplings to $b\bar{b}$.

Radiative Corrections to MSSM Higgs Masses and Couplings

Radiative corrections can have a significant impact on the values of Higgs boson masses and couplings in the MSSM. Important contributions come from loops of SM particles as well as their supersymmetric partners. The dominant effects arise from the incomplete cancellation between top and scalar-top (stop) loops. The stop and sbottom masses and mixing angles depend on the supersymmetric Higgsino mass parameter μ and on the soft-supersymmetry-breaking parameters [102]: M_Q , M_U , M_D , A_t and A_b , where the first three are the left-chiral and the two right-chiral top and bottom scalar quark mass parameters, respectively, and the last two are the trilinear parameters that enter the off-diagonal squark mixing elements: $X_t \equiv A_t - \mu \cot\beta$ and $X_b \equiv A_b - \mu \tan\beta$. The corrections affecting the Higgs boson masses, production, and decay properties depend on all of these parameters. For simplicity, we shall initially assume that A_t , A_b , and μ are real parameters. The impact of complex

phases on MSSM parameters, which will induce CP -violation in the Higgs sector, is addressed below.

Radiative corrections to the Higgs boson masses have been computed using a number of techniques, with a variety of approximations; see Refs. [106] through [116]. They depend strongly on the top quark mass ($\sim m_t^4$) and the stop mixing parameter X_t , and there is also a logarithmic dependence on the stop masses. For large $\tan\beta$, effects from the bottom-sbottom sector are also relevant. One of the most striking effects is the increase of the upper bound of the light CP -even Higgs boson mass, as first noted in [106,107]. The value of m_h is maximized for large $m_A \gg M_Z$, when all other MSSM parameters are fixed. Moreover, $\tan\beta \gg 1$ also maximizes m_h , when all other parameters are held fixed. Taking m_A large (the decoupling limit) and $\tan\beta \gg 1$, the value of m_h can be further maximized at one-loop level for $X_t \simeq \sqrt{6}M_{\text{SUSY}}$, where $M_{\text{SUSY}} \simeq M_Q \simeq M_U \simeq M_D$ is an assumed common value of the soft SUSY-breaking squark mass parameters. This choice of X_t is called the “maximal-mixing scenario” which will be indicated by m_h -max. Instead, for $X_t = 0$, which is called the “no-mixing scenario,” the value of m_h has its lowest possible value, for fixed m_A and all other MSSM parameters. The value of m_h also depends on the specific value of M_{SUSY} and μ and more weakly on the electroweak gaugino mass as well as the gluino mass at two-loop level. For example, raising M_{SUSY} from 1 TeV to 2 TeV can increase m_h by 2-5 GeV. Variation of the value of m_t by 1 GeV changes the value of m_h by about the same amount. For any given scenario defined by a full set of MSSM parameters, we will denote the maximum value of m_h by $m_h^{\text{max}}(\tan\beta)$, for each value of $\tan\beta$. Allowing for the experimental uncertainty on m_t and for the uncertainty inherent in the theoretical analysis, one finds for $M_{\text{SUSY}} \lesssim 2$ TeV, large m_A and $\tan\beta \gg 1$, $m_h^{\text{max}} = 135$ GeV in the m_h -max scenario, and $m_h^{\text{max}} = 122$ GeV in the no-mixing scenario [117,118]. In practice, parameter values leading to maximal mixing are not obtained in most models of supersymmetry breaking, so typical upper limits on m_h will lie between these two extremes [119]. The relatively small mass of the lightest neutral scalar boson is a prediction for both

the CP -conserving (CPC) and CP -violating (CPV) [120] scenarios, which emphasizes the importance of the searches at currently running and future accelerators.

Radiative corrections also modify significantly the values of the Higgs boson couplings to fermion pairs and to vector boson pairs. The tree-level Higgs couplings depend strongly on the value of $\cos(\beta - \alpha)$. In a first approximation, when radiative corrections of the Higgs squared-mass matrix are computed, the diagonalizing angle α is shifted from its tree-level value, and hence one may compute a “radiatively-corrected” value for $\cos(\beta - \alpha)$. This shift provides one important source of the radiative corrections to the Higgs couplings. In particular, depending on the sign of μX_t and the magnitude of X_t/M_{SUSY} , modifications of α can lead to important variations of the SM-like Higgs boson coupling to bottom quarks and tau leptons [115]. Additional contributions from the one-loop vertex corrections to tree-level Higgs couplings must also be considered [111,121–127]. These contributions alter significantly the Higgs-fermion Yukawa couplings at large $\tan\beta$, both in the neutral and charged Higgs sector. Moreover, these radiative corrections can modify the basic relationship $g_{h,H,A b\bar{b}}/g_{h,H,A\tau^+\tau^-} \propto m_b/m_\tau$, and change the main features of MSSM Higgs phenomenology.

Decay Properties of MSSM Higgs Bosons

In the MSSM, neglecting CP -violating effects, one must consider the decay properties of three neutral Higgs bosons and one charged Higgs pair. In the region of parameter space where $m_A \gg m_Z$ and the masses of supersymmetric particles are large, the decoupling limit applies, and the decay rates of h into SM particles are nearly indistinguishable from those of the SM Higgs boson. Hence, the h boson will decay mainly to fermion pairs, since the mass, less than about 135 GeV, is far below the W^+W^- threshold. The SM-like branching ratios of h are modified if decays into supersymmetric particles are kinematically allowed [128]. In addition, if light superpartners exist that can couple to photons and/or gluons, then the decay rates to gg and $\gamma\gamma$ could deviate from the corresponding SM rates. In the decoupling limit, the heavier Higgs states, H , A and H^\pm , are roughly mass degenerate, and their decay

branching ratios strongly depend on $\tan\beta$ as shown below. The AWW and AZZ couplings vanish, and the HWW and HZZ couplings are very small. For values of $m_A \sim \mathcal{O}(M_Z)$, all Higgs boson states lie below 200 GeV in mass. In this parameter regime, there is a significant area of the parameter space in which none of the neutral Higgs boson decay properties approximates that of the SM Higgs boson. For $\tan\beta \gg 1$, the resulting Higgs phenomenology shows marked differences from that of the SM Higgs boson [129] and significant modifications to the $b\bar{b}$ and/or the $\tau^+\tau^-$ decay rates may occur via radiative effects.

After incorporating the leading radiative corrections to Higgs couplings from both QCD and supersymmetry, the following decay features are relevant in the MSSM. The decay modes $h, H, A \rightarrow b\bar{b}, \tau^+\tau^-$ dominate the neutral Higgs boson decay modes when $\tan\beta$ is large for all values of the Higgs boson masses. For small $\tan\beta$, these modes are significant for neutral Higgs boson masses below $2m_t$ (although there are other competing modes in this mass range), whereas the $t\bar{t}$ decay mode dominates above its kinematic threshold. In contrast to the SM Higgs boson, the vector boson decay modes of H are strongly suppressed at large m_H due to the suppressed HVV couplings in the decoupling limit. For the charged Higgs boson, $H^+ \rightarrow \tau^+\nu_\tau$ dominates below $t\bar{b}$ threshold, while $H^+ \rightarrow t\bar{b}$ dominates for large values of m_{H^\pm} . For low values of $\tan\beta$ ($\lesssim 1$) and low values of the charged Higgs boson mass ($\lesssim 120$ GeV), the decay mode $H^+ \rightarrow c\bar{s}$ becomes relevant.

In addition to the decay modes of the neutral Higgs bosons into fermion and gauge boson final states, additional decay channels may be allowed which involve scalars of the extended Higgs sector, *e.g.*, $h \rightarrow AA$. Supersymmetric final states from Higgs boson decays into charginos, neutralinos and third-generation squarks and sleptons can be important if they are kinematically allowed [130]. One interesting possibility is a significant branching ratio for the decay of a neutral Higgs boson to the invisible mode $\tilde{\chi}_1^0\tilde{\chi}_1^0$ (where the lightest neutralino $\tilde{\chi}_1^0$ is the lightest supersymmetric particle) [131], which poses a significant challenge at hadron colliders.

Searches for Neutral Higgs Bosons (CPC Scenario)

Most of the experimental investigations carried out at LEP and the Tevatron assume CP -conservation (*CPC*) in the MSSM Higgs sector. In many cases the search results are interpreted in a number of specific benchmark models where a representative set of the relevant SUSY breaking parameters are specified [117]. Some of these parameter choices illustrate scenarios in which the detection of Higgs bosons at LEP or in hadron collisions is experimentally challenging due to the limited phase space or the suppression of the main discovery channels. For instance, the m_h -max scenario defined above maximizes the allowed values of m_h , for a given $\tan\beta$, M_{SUSY} , and m_t , leading to relatively conservative exclusion limits.

Searches for Neutral MSSM Higgs Bosons at LEP

In e^+e^- collisions at LEP energies, the main production mechanisms of the neutral MSSM Higgs bosons are the Higgs-strahlung processes $e^+e^- \rightarrow hZ$, HZ and the pair production processes $e^+e^- \rightarrow hA$, HA , while the fusion processes play a marginal role. The cross sections can be expressed in terms of the SM cross section and the parameters α and β introduced above. For the light CP -even Higgs boson h the following expressions hold, in good approximation,

$$\sigma_{hZ} = \sin^2(\beta - \alpha) \sigma_{hZ}^{\text{SM}}, \quad \sigma_{hA} = \cos^2(\beta - \alpha) \bar{\lambda} \sigma_{hZ}^{\text{SM}}$$

where σ_{hZ}^{SM} stands for a SM cross section with a SM Higgs boson of mass equal to m_h . The phase space functions are

$$\bar{\lambda} = \lambda_{Ah}^{3/2} / \left[\lambda_{Zh}^{1/2} (12M_Z^2/s + \lambda_{Zh}) \right]$$

and $\lambda_{ij} = [1 - (m_i + m_j)^2/s][1 - (m_i - m_j)^2/s]$, where s is the square of the e^+e^- collision energy. These Higgs-strahlung and pair production cross sections are complementary since $\sin^2(\beta - \alpha) + \cos^2(\beta - \alpha) = 1$. The cross sections for the heavy scalar boson H are obtained by interchanging $\sin^2(\beta - \alpha)$ and $\cos^2(\beta - \alpha)$ and replacing the index h by H in the above expressions, and by defining σ_{HZ}^{SM} similarly to σ_{hZ}^{SM} . The Higgs-strahlung process $e^+e^- \rightarrow hZ$ is relevant for large $m_A > m_h^{\text{max}}(\tan\beta)$ or low $m_A < m_h^{\text{max}}(\tan\beta)$ and low $\tan\beta$; while the

pair-production process $e^+e^- \rightarrow hA$ is relevant for low $m_A < m_h^{\max}(\tan\beta)$.

The searches at LEP exploit the complementarity between the Higgs-strahlung process $e^+e^- \rightarrow hZ$, and the pair-production process $e^+e^- \rightarrow hA$. In addition, when $m_A < m_h^{\max}(\tan\beta)$, the H boson has SM-like couplings to the Z boson, so if kinematically allowed, $e^+e^- \rightarrow Hz$ is also considered. For Higgs-strahlung, the searches for the SM Higgs boson are re-interpreted, taking into account the MSSM reduction factor $\sin^2(\beta - \alpha)$ for h ($\cos^2(\beta - \alpha)$ for H). For pair production, dedicated searches are performed for the $(b\bar{b})(b\bar{b})$ and $(\tau^+\tau^-)(q\bar{q})$ final states.

The limits from the four LEP experiments are described in Refs. [54,55,132,133]. The combined LEP data did not reveal any excess of events which would indicate the production of Higgs bosons, and combined limits were derived [18]. These limits are shown in Fig. 9 for the m_h -max scenario, in the $(m_h, \tan\beta)$ parameter plane (see Ref. 18 for other projections and other benchmark models). For values of $\tan\beta$ below ~ 5 or for $m_A \gg M_Z$ and high values of $\tan\beta$, the limit on m_h is nearly that of the SM searches, as $\sin^2(\beta - \alpha) \approx 1$. For higher values of $\tan\beta$, the $e^+e^- \rightarrow hA$ searches become the most important, and they do not set as stringent a limit on m_h . In this scenario, the 95% C.L. mass bounds are $m_h > 92.8$ GeV and $m_A > 93.4$ GeV, and values of $\tan\beta$ from 0.7 to 2.0 are excluded taking $m_t = 174.3$ GeV. This excluded $\tan\beta$ range depends on M_{SUSY} and m_t ; larger values of either of these masses increase the Higgs boson mass, and reduce the excluded range of $\tan\beta$. Furthermore, the uncertainty on the SM-like Higgs boson mass from higher-order corrections, which were not included in the current analysis, is about 3 GeV [118].

The neutral Higgs bosons may also be produced by Yukawa processes $e^+e^- \rightarrow f\bar{f}\phi$, where the Higgs particle $\phi \equiv h, H, A$, is radiated off a massive fermion ($f \equiv b$ or τ^\pm). These processes can be dominant at low masses, and whenever the $e^+e^- \rightarrow hZ$ and hA processes are suppressed. The corresponding ratios of the $f\bar{f}h$ and $f\bar{f}A$ couplings to the SM coupling are $\sin\alpha/\cos\beta$ and $\tan\beta$, respectively. The LEP data have been used to

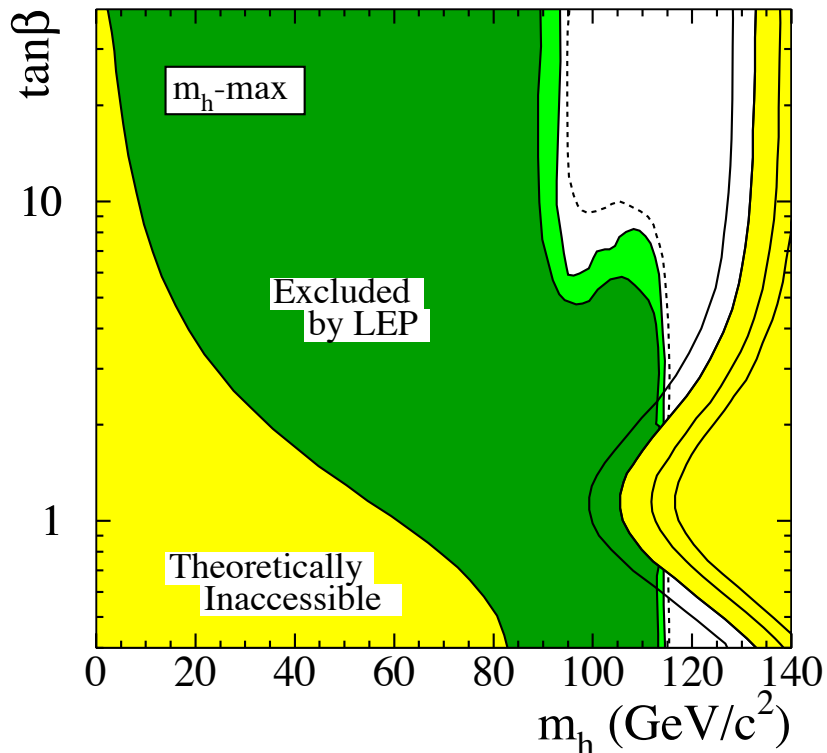


Figure 9: The MSSM exclusion contours, at 95% C.L. (light-green) and 99.7% CL (dark-green), obtained by LEP for the *CPC* m_h -max benchmark scenario, with $m_t = 174.3$ GeV. The figure shows the excluded and theoretically inaccessible regions in the $(m_h, \tan \beta)$ projection. The upper edge of the theoretically allowed region is sensitive to the top quark mass; it is indicated, from left to right, for $m_t = 169.3, 174.3, 179.3$ and 183.0 GeV. The dashed lines indicate the boundaries of the regions which are expected to be excluded on the basis of Monte Carlo simulations with no signal (from Ref. 18). Color version at end of book.

search for $b\bar{b}b\bar{b}$, $b\bar{b}\tau^+\tau^-$, and $\tau^+\tau^-\tau^+\tau^-$ final states [134,135]. Regions of low mass and high enhancement factors are excluded by these searches.

Searches for Neutral MSSM Higgs Bosons at Hadron Colliders

The production mechanisms for the SM Higgs boson at hadron colliders can also be relevant for the production of the MSSM neutral Higgs bosons. However, one must take into

account the possibility of enhanced or suppressed couplings with respect to those of the Standard Model, since these can significantly modify the production cross sections of neutral Higgs bosons. The supersymmetric-QCD corrections due to the exchange of virtual squarks and gluinos may modify the cross sections depending on the values of these supersymmetric particle masses. The MSSM neutral Higgs boson production cross sections at hadron colliders have been computed in Refs. [115,127,136].

Over a large fraction of the MSSM parameter space, one of the CP -even neutral Higgs bosons (h or H) couples to the vector bosons with SM-like strength and has a mass below 135 GeV. As shown in the SM Higgs section above (Fig. 6), the current searches for SM-like Higgs bosons at the Tevatron are not yet able to cover that mass range. However, if the expected improvements in sensitivity are achieved, the regions of MSSM parameter space in which one of these two scalars behaves like the SM Higgs will also be probed [137,138].

Scenarios with enhanced Higgs boson production cross sections are studied at the Tevatron. The best sensitivity is in the regime with low to moderate m_A and with large $\tan\beta$ which enhances the couplings of the Higgs bosons to down-type fermions. The corresponding limits on the Higgs boson production cross section times the branching ratio of the Higgs boson into down-type fermions can be interpreted in MSSM benchmark scenarios [139]. If $\phi = A, H$ for $m_A > m_h^{\max}$, and $\phi = A, h$ for $m_A < m_h^{\max}$, the most promising channels at the Tevatron are $b\bar{b}\phi, \phi \rightarrow b\bar{b}$ or $\phi \rightarrow \tau^+\tau^-$, with three tagged b -jets or $b\tau\tau$ in the final state, respectively, and the inclusive $p\bar{p} \rightarrow \phi \rightarrow \tau^+\tau^-$ process, with contributions from both $gg \rightarrow \phi$ and $b\bar{b}\phi$ production. Although Higgs boson production via gluon fusion has a higher cross section than via associated production, it cannot be used to study the $\phi \rightarrow b\bar{b}$ decay mode since the signal is overwhelmed by QCD background.

The CDF and D \emptyset collaborations have searched for neutral Higgs bosons produced in association with bottom quarks and which decay into $b\bar{b}$ [140–142], or into $\tau^+\tau^-$ [143]. The most recent searches in the $b\bar{b}\phi$ channel with $\phi \rightarrow b\bar{b}$ analyze

approximately 2.5 fb^{-1} of data (CDF) and 2.6 fb^{-1} ($D\bar{\emptyset}$). Dedicated triggers are used to collect the data samples, but the multijet QCD background remains very large. These triggers require the presence of at least three jets, and also require tracks reconstructed with large impact parameters which point near calorimeter energy deposits. The data are analyzed by requiring three well-separated jets with reconstructed secondary vertices indicating the presence of B hadrons. The distribution of the invariant mass of the two leading jets would be more sharply peaked for the Higgs boson signal than for the background. The QCD background rates and shapes are inferred from data control samples, in particular, the sample with two b tagged jets and a third, untagged jet. Monte Carlo models are used to estimate the biases on the shapes of the background predictions due to the requirement of a third b tag. Separate signal hypotheses are tested and limits are placed on $\sigma(p\bar{p} \rightarrow b\bar{b}\phi) \times \text{BR}(\phi \rightarrow b\bar{b})$. Fig. 10 shows the upper limits from CDF and $D\bar{\emptyset}$ assuming that the decay widths of the Higgs bosons are small compared with the experimental resolution.

CDF and $D\bar{\emptyset}$ have also performed searches for inclusive production of Higgs bosons with subsequent decays to $\tau^+\tau^-$ using dedicated triggers designed for these searches [144–146]. Tau leptons are more difficult to identify than jets containing B hadrons, as only some of the possible τ lepton decays are sufficiently distinct from the jet backgrounds. Both CDF and $D\bar{\emptyset}$ search for pairs of isolated tau leptons; one of the tau leptons is required to decay leptonically (either to an electron and two neutrinos, or a muon and two neutrinos), while the other tau may decay either leptonically or hadronically. Requirements placed on the energies and angles of the visible tau decay products help to reduce the background from $W+\text{jets}$ processes, where a jet is falsely reconstructed as a tau lepton. The dominant remaining background process is $Z \rightarrow \tau^+\tau^-$, which can be separated from a Higgs boson signal by using the invariant mass of the observed decay products of the tau leptons. Fig. 10 shows the limits on $\sigma(p\bar{p} \rightarrow \phi + X) \times \text{BR}(\phi \rightarrow \tau^+\tau^-)$ for the CDF and $D\bar{\emptyset}$ searches, which use 1.8 and 2.2 fb^{-1} of data, respectively. Fig. 10 also shows the combination [147] of

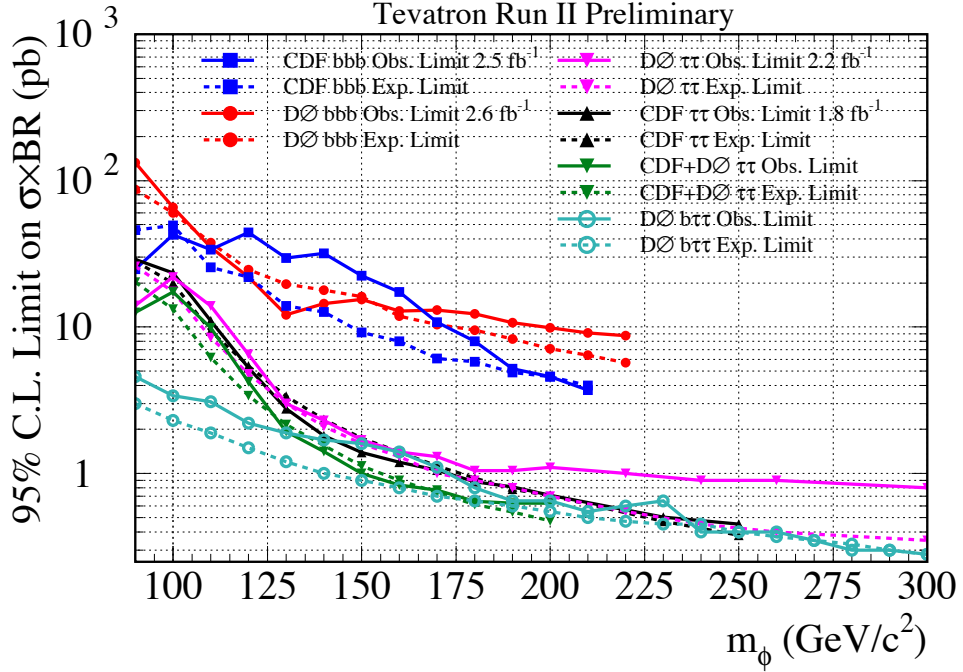


Figure 10: The 95% C.L. limits on $\sigma(b\bar{b}\phi) \times \text{BR}(\phi \rightarrow b\bar{b})$ and $\sigma(\phi + X) \times \text{BR}(\phi \rightarrow \tau^+\tau^-)$ from the Tevatron collaborations. The DØ limit on $\sigma(b\bar{b}\phi) \times \text{BR}(\phi \rightarrow \tau^+\tau^-)$ and the Tevatron combined limit on $\sigma(\phi + X) \times \text{BR}(\phi \rightarrow \tau^+\tau^-)$ are also shown. The observed limits are indicated with solid lines, and the expected limits are indicated with dashed lines. The limits are to be compared with the sum of signal predictions for Higgs bosons with similar masses. The decay widths of the Higgs bosons are assumed to be much smaller than the experimental resolution. Color version at end of book.

CDF and DØ's search results in the tau-pair decay mode, for Higgs boson masses tested by both collaborations. The decay widths of the Higgs bosons are assumed to be small compared with the experimental resolution, which is much broader in the tau channels than in the $b\bar{b}\phi$ search, due to the presence of energetic neutrinos in the tau decay products.

In order to interpret the experimental data in terms of MSSM benchmark scenarios, it is necessary to consider carefully the effect of radiative corrections on the production and decay processes. The bounds from the $b\bar{b}\phi, \phi \rightarrow b\bar{b}$ channel

depend strongly on the radiative corrections affecting the relation between the bottom quark mass and the bottom Yukawa coupling. In the channels with $\tau^+\tau^-$ final states, however, compensations occur between large corrections in the Higgs boson production and decay. The total production rate of bottom quarks and τ pairs mediated by the production of a CP -odd Higgs boson in the large $\tan\beta$ regime is approximately given by

$$\begin{aligned}\sigma(b\bar{b}A) \times \text{BR}(A \rightarrow b\bar{b}) &\simeq \\ \sigma(b\bar{b}A)_{\text{SM}} \frac{\tan^2\beta}{(1 + \Delta_b)^2} \frac{9}{(1 + \Delta_b)^2 + 9},\end{aligned}$$

and

$$\begin{aligned}\sigma(gg \rightarrow A, b\bar{b}A) \times \text{BR}(A \rightarrow \tau^+\tau^-) &\simeq \\ \sigma(gg \rightarrow A, b\bar{b}A)_{\text{SM}} \frac{\tan^2\beta}{(1 + \Delta_b)^2 + 9},\end{aligned}$$

where $\sigma(b\bar{b}A)_{\text{SM}}$ and $\sigma(gg \rightarrow A, b\bar{b}A)_{\text{SM}}$ denote the values of the corresponding SM Higgs boson cross sections for a SM Higgs boson mass equal to m_A . The function Δ_b includes the dominant effects of SUSY radiative corrections for large $\tan\beta$ [125,126]. The main radiative contributions in Δ_b depend strongly on $\tan\beta$ and on the SUSY mass parameters [115]. The $b\bar{b}A$ channel is more sensitive to the value of Δ_b through the factor $1/(1 + \Delta_b)^2$ than the inclusive $\tau^+\tau^-$ channel, for which this leading dependence on Δ_b cancels out. As a consequence, the limits derived from the inclusive $\tau^+\tau^-$ channel depend less on the precise MSSM scenario chosen than those of the $b\bar{b}A$ channel.

The production and decay rates of the CP -even Higgs bosons with $\tan\beta$ -enhanced couplings to down-type fermions – H (or h) for m_A larger (or smaller) than m_h^{\max} , respectively – are governed by formulae similar to the ones presented above. At high $\tan\beta$, one of the CP -even and the CP -odd Higgs bosons are nearly degenerate in mass, enhancing the signal cross section by roughly a factor of two, without complicating the experimental signature except in a small mass region in which the three neutral MSSM Higgs boson masses are close together and each boson contributes to the total production rate. A detailed discussion of the impact of radiative corrections in these search modes is presented in Ref. 139.

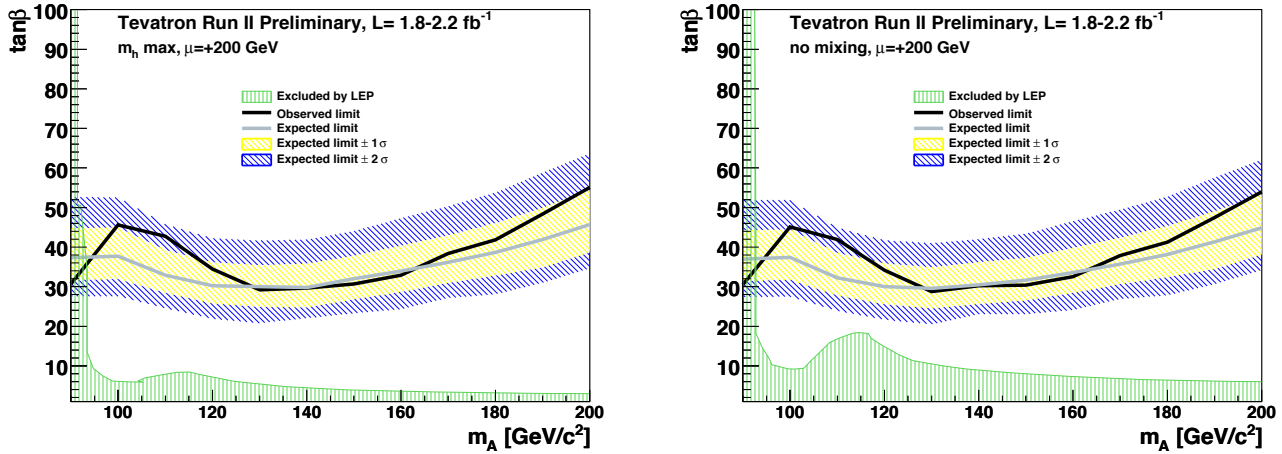


Figure 11: The 95% C.L. MSSM exclusion contours obtained by a combination of the CDF and DØ searches for $H \rightarrow \tau^+\tau^-$ in the m_h -max (left) and *no-mixing* (right) benchmark scenarios, both with $\mu = 200$ GeV, projected onto the $(m_A, \tan\beta)$ plane [147]. The regions above the solid black line are excluded, and the shaded and hatched bands centered on the lighter line show the distributions of expected exclusions in the absence of a signal. Also shown are the regions excluded by LEP searches [18], assuming a top quark mass of 174.3 GeV. The Tevatron results are not sensitive to the precise value of the top quark mass. Color version at end of book.

The excluded domain in the $(m_A, \tan\beta)$ projection for the combination of CDF and DØ’s inclusive $\phi \rightarrow \tau^+\tau^-$ searches [147] are shown in Fig. 11. The searches consider the contribution of both the *CP*-odd and *CP*-even neutral Higgs bosons with enhanced couplings to bottom quarks. The excluded regions are shown in the m_h -max and *no-mixing* benchmark scenarios, with $\mu = 200$ GeV. The $bbb(b)$ searches are somewhat less sensitive, typically yielding expected upper limits on $\tan\beta$ of 60 and above due to higher QCD backgrounds, sensitivity to the Higgs boson width, and the Δ_{ab} corrections.

The sensitivity of the Tevatron searches will improve with the continuously growing data samples and with the combination of all channels of both experiments. The small backgrounds in the $\tau^+\tau^-$ channels, and the fact that better exclusions in the $bbb(b)$ channel imply narrower Higgs boson decay widths, which feeds back to improve the sensitivity of the searches, mean that the limits on the cross sections are expected to improve faster than $1/\sqrt{\mathcal{L}}$, where \mathcal{L} is the integrated luminosity. Eventually, $\tan\beta$ down to about 20 should be tested for values of m_A up to a few hundred GeV. By the end of Run II, the Tevatron searches for the associated production of a SM Higgs boson in $W^\pm H$ and ZH channels may have a strong impact on the excluded domains in Fig. 11. The combination of the LEP and Tevatron searches is expected to probe vast regions of the $(m_A, \tan\beta)$ plane.

Searches for charged Higgs bosons at the Tevatron are presented in Section IV, in the more general framework of the 2HDM.

Prospects for discovering the MSSM Higgs bosons at the LHC have been explored in detail at $\sqrt{s} = 14$ TeV; see Refs. [93,21] for reviews of these studies. They predict that the reach of the LHC experiments would be sufficient to discover MSSM Higgs bosons in many different channels. The main channels for the SM-like Higgs boson are expected to be $q\bar{q}\phi \rightarrow q\bar{q}\tau^+\tau^-$ and inclusive $\phi \rightarrow \gamma\gamma$, where $\phi = h$ or H , depending on m_A . The discovery of a light SM-like Higgs boson with $m_h < 130$ GeV would require a few years of running. With an integrated luminosity larger than 30 fb^{-1} , the $t\bar{t}\phi$ production process may become effective. For non-SM-like MSSM Higgs bosons, the most relevant channels are expected to be $pp \rightarrow H/A + X$, with $H/A \rightarrow \tau^+\tau^-$ and $pp \rightarrow tH^\pm + X$ with $H^\pm \rightarrow \tau\nu_\tau$ [137]. After the inclusion of supersymmetric radiative corrections to the production cross sections and decay widths [139,148], the prospective discovery reach in these channels is robust, with mild dependence on the specific MSSM parameters.

Effects of CP Violation on the MSSM Higgs Spectrum

In the Standard Model, CP -violation (CPV) is induced by phases in the Yukawa couplings of the quarks to the Higgs field, which results in one non-trivial phase in the CKM mixing matrix. SUSY scenarios with new CPV phases are theoretically appealing, since additional CPV beyond that observed in the K and B meson systems is required to explain the observed cosmic matter-antimatter asymmetry [149,150]. In the MSSM, there are additional sources of CPV from phases in the various supersymmetric mass parameters. In particular, the gaugino mass parameters (M_i , $i = 1, 2, 3$), the Higgsino mass parameter, μ , the bilinear Higgs squared-mass parameter, m_{12}^2 , and the trilinear couplings of the squark and slepton fields (\tilde{f}) to the Higgs fields, A_f , may carry non-trivial phases. The two parameter combinations $\arg[\mu A_f(m_{12}^2)^*]$ and $\arg[\mu M_i(m_{12}^2)^*]$ are invariant under phase redefinitions of the MSSM fields [151,152]. Therefore, if one of these quantities is non-zero, there would be new sources of CP -violation, which affects the MSSM Higgs sector through radiative corrections [120,152–157]. The mixing of the neutral CP -odd and CP -even Higgs boson states is no longer forbidden. Hence, m_A is no longer a physical parameter. However, the charged Higgs boson mass m_{H^\pm} is still physical and can be used as an input for the computation of the neutral Higgs spectrum of the theory.

For large values of m_{H^\pm} , corresponding to the decoupling limit, the properties of the lightest neutral Higgs boson state approach those of the SM Higgs boson. That is, for $m_{H^\pm} \gg M_W$, the lightest neutral Higgs boson is approximately a CP -even state, with CPV couplings that are suppressed by terms of $\mathcal{O}(m_W^2/m_{H^\pm}^2)$. In particular, the upper bound on the lightest neutral Higgs boson mass, takes the same value as in the CP -conserving case [152]. Nevertheless, there still can be significant mixing between the two heavier neutral mass eigenstates. For a detailed study of the Higgs boson mass spectrum and parametric dependence of the Higgs boson mass radiative corrections, see Ref. [153,156].

Major variations to the MSSM Higgs phenomenology occur in the presence of explicit CPV phases. In the CPV case,

vector boson pairs couple to all three neutral Higgs boson mass eigenstates, H_i ($i = 1, 2, 3$), with couplings

$$g_{H_i VV} = \cos \beta \mathcal{O}_{1i} + \sin \beta \mathcal{O}_{2i}$$

$$g_{H_i H_j Z} = \mathcal{O}_{3i}(\cos \beta \mathcal{O}_{2j} - \sin \beta \mathcal{O}_{1j}) - \mathcal{O}_{3j}(\cos \beta \mathcal{O}_{2i} - \sin \beta \mathcal{O}_{1i})$$

where the $g_{H_i VV}$ couplings are normalized to the analogous SM coupling and the $g_{H_i H_j Z}$ have been normalized to $g_Z^{\text{SM}}/2$. \mathcal{O}_{ij} is the orthogonal matrix relating the weak eigenstates to the mass eigenstates. It has non-zero off-diagonal entries mixing the CP -even and CP -odd components of the weak eigenstates. The above couplings obey the relations

$$\sum_{i=1}^3 g_{H_i ZZ}^2 = 1 \quad \text{and} \quad g_{H_k ZZ} = \varepsilon_{ijk} g_{H_i H_j Z}$$

where ε_{ijk} is the Levi-Civita symbol.

Another consequence of CPV effects in the scalar sector is that all neutral Higgs bosons can couple to both scalar and pseudoscalar fermion bilinear densities. The couplings of the mass eigenstates H_i to fermions depend on the loop-corrected fermion Yukawa couplings (similarly to the CPC case), on $\tan \beta$ and on the \mathcal{O}_{ji} . The resulting expressions for the scalar and pseudoscalar components of the neutral Higgs boson mass eigenstates to fermions and the charged Higgs boson to fermions are given in Refs. [153,158].

Regarding their decay properties, the lightest mass eigenstate, H_1 , predominantly decays to $b\bar{b}$ if kinematically allowed, with a smaller fraction decaying to $\tau^+\tau^-$, similar to the CPC case. If kinematically allowed, a SM-like neutral Higgs boson, H_2 or H_3 can decay predominantly to $H_1 H_1$; otherwise it will decay preferentially to $b\bar{b}$.

Searches for Neutral Higgs Bosons in CPV Scenarios

In CPV MSSM scenarios, the three neutral Higgs eigenstates H_i do not have well-defined CP quantum numbers; they all could be produced by Higgs-strahlung, $e^+e^- \rightarrow H_i Z$, and in pairs, $e^+e^- \rightarrow H_i H_j$ ($i \neq j$), with rates which depend on the details of the CPV scenario. Possible cascade decays such as

H_2 or $H_3 \rightarrow H_1 H_1$ can lead to interesting experimental signatures in the Higgs-strahlung processes, $e^+ e^- \rightarrow H_2 Z$ or $H_3 Z$. For wide ranges of the model parameters, the lightest neutral Higgs boson H_1 has a predicted mass that would be accessible at LEP, if it would couple to the Z boson with SM-like strength. The second- and third-lightest Higgs bosons H_2 and H_3 may have been either out of reach, or may have had small cross sections. Altogether, the searches in the CPV MSSM scenario are experimentally more difficult, and hence have a weaker sensitivity.

The cross section for the Higgs-strahlung and pair production processes are given by [120,152,153,157]

$$\sigma_{H_i Z} = g_{H_i ZZ}^2 \sigma_{H_i Z}^{\text{SM}} \quad \sigma_{H_i H_j} = g_{H_i H_j Z}^2 \bar{\lambda} \sigma_{H_i Z}^{\text{SM}}.$$

In the expression of $\bar{\lambda}$, defined for the CPC case, the indices h and A are to be replaced by H_i and H_j , respectively, $\sigma_{H_i Z}^{\text{SM}}$ stands for the SM cross section for a SM Higgs boson with a mass equal to m_{H_i} , and the couplings are defined above in term of the orthogonal matrix relating the weak eigenstates to the mass eigenstates.

The Higgs boson searches at LEP were interpreted [18] in a CPV benchmark scenario [120] for which the parameters were chosen so as to maximize the phenomenological differences with respect to the CPC scenario. This scenario, called CPX, is specified by $|A_t| = |A_b| = 1000$ GeV, $\phi_A = \phi_{m_{\tilde{g}}} = \pi/2$, $\mu = 2$ TeV, and $M_{\text{SUSY}} = 500$ GeV. Fig. 12 shows the exclusion limits of LEP in the $(m_{H_1}, \tan \beta)$ plane for $m_t = 174.3$ GeV. Values of $\tan \beta$ less than about 3 are excluded in this scenario. However, no absolute lower bound can be set for the mass of the lightest neutral Higgs boson H_1 , for an updated study see Ref. [159]. Similar exclusion plots, for other choices of model parameters, can be found in Ref. [18]. The Tevatron CP -conserving results and projection for MSSM Higgs searches, as well as the existing projections for LHC MSSM CP -conserving searches have been reinterpreted in the framework of CP -violating MSSM Higgs in Ref. 138. The CPX scenario was also studied by ATLAS and CMS collaborations.

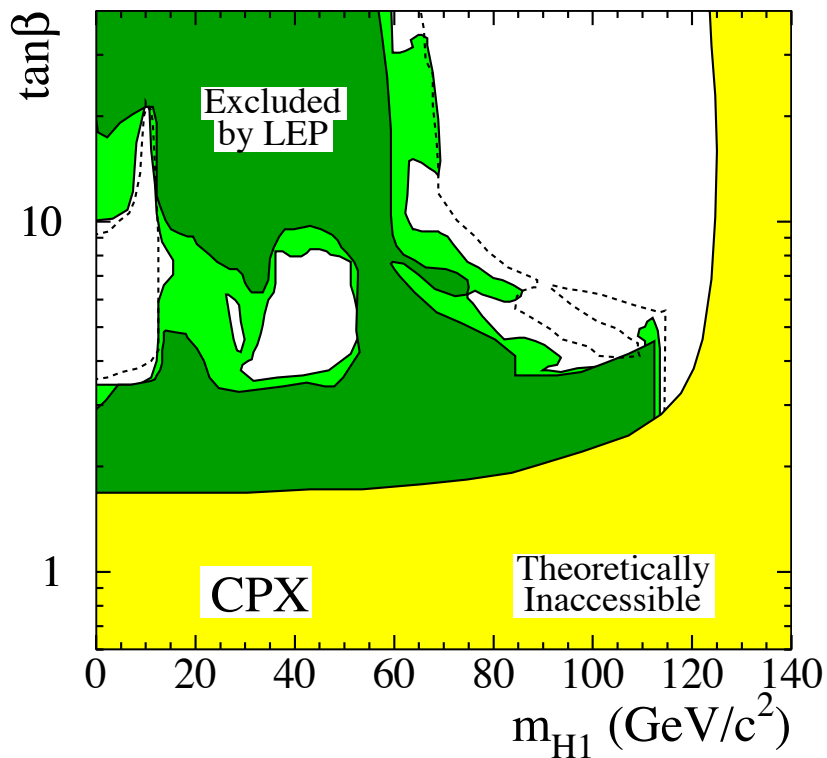


Figure 12: The MSSM exclusion contours, at the 95% C.L. (light-green) and the 99.7% CL (dark-green), obtained by LEP for the CPX scenario defined in the text. Here, $m_t = 174.3$ GeV. The figure shows the excluded and theoretically inaccessible regions in the $(m_{H_1}, \tan \beta)$ projection. The dashed lines indicate the boundary of the region which is expected to be excluded at the 95% C.L. in the absence of a signal. Color version at end of book.

Indirect Constraints from Electroweak and B-physics Observables and Dark Matter Searches

Indirect bounds from a global fit to precision measurements of electroweak observables can be derived in terms of MSSM parameters [160] in a way similar to what was done in the SM. The minimum χ^2 for the MSSM fit is slightly lower than what is obtained for the SM, and the fit accommodates a low value of the lightest Higgs boson mass which is a prediction of the MSSM [161]. Given the MSSM and SM predictions for M_W as

a function of m_t , and varying the Higgs boson mass and the SUSY spectrum, one finds that the MSSM overlaps with the SM when SUSY masses are large, of $\mathcal{O}(2 \text{ TeV})$, and the light SM-like Higgs boson has a mass close to the experimental bound of 114.4 GeV. The MSSM Higgs boson mass expectations are compatible with the constraints provided by the measurements of m_t and M_W [162].

Improvements in our understanding of B -physics observables put indirect constraints on MSSM scenarios in regions in which Higgs boson searches at the Tevatron and the LHC are sensitive. In particular, $\text{BR}(B_s \rightarrow \mu^+ \mu^-)$, $\text{BR}(b \rightarrow s\gamma)$, and $\text{BR}(B_u \rightarrow \tau\nu)$ play an important role within minimal flavor-violating (MFV) models [163], in which flavor effects are induced by loop factors proportional to the CKM matrix elements, as in the SM. For example, see Refs. [137,164,165,166]. The supersymmetric contributions to these observables come both at the tree- and loop-level, and have a different parametric dependence, but share the property that they become significant for large values of $\tan\beta$, which is also the regime in which searches for non-standard MSSM Higgs bosons at hadron colliders become relevant. The recent measurement of ΔM_s and the CP-odd phase ϕ_s by the CDF and DØ collaborations [167,168,169] could also have implications for MSSM Higgs physics.

In the SM, the relevant contributions to the rare decay $B_s \rightarrow \mu^+ \mu^-$ come through the Z -penguin and the W^\pm -box diagrams [172]. In supersymmetry with large $\tan\beta$, there are also significant contributions from Higgs-mediated neutral currents [173,174,175,176], which grow with the sixth power of $\tan\beta$ and decrease with the fourth power of the CP -odd Higgs boson mass m_A . Therefore, the upper limits from the Tevatron [170] put strong restrictions on possible flavor-changing neutral currents (FCNC) in the MSSM at large $\tan\beta$.

Further constraints are obtained from the rare decay $b \rightarrow s\gamma$. The SM rate is known up to NNLO corrections [177,179] and is in good agreement with measurements [178]. In the minimal flavor-violating MSSM, there are new contributions from charged Higgs and chargino-stop diagrams. The charged

Higgs boson's contribution is enhanced for small values of its mass and can be partially canceled by the chargino contribution or by higher-order $\tan\beta$ -enhanced loop effects.

The branching ratio $B_u \rightarrow \tau\nu$, measured by the Belle [180] and BaBar [181] collaborations, also constrains the MSSM. The SM expectation is in slight tension with the latest experimental results [6]. In the MSSM, there is an extra tree-level contribution from the charged Higgs which interferes destructively with the SM contribution, and which increases for small values of the charged Higgs boson mass and large values of $\tan\beta$ [182]. Charged Higgs effects on $B \rightarrow D\tau\nu$ decays [183,184], constrain in an important way the parameter space region for small values of the charged Higgs boson mass and large values of $\tan\beta$, that is compatible with measured values of $B_u \rightarrow \tau\nu$ [185,186,6].

Several studies [137,164–166,187] have shown that, in extended regions of parameter space, the combined B -physics measurements impose strong constraints on the MSSM models to which Higgs boson searches at the Tevatron and the LHC are sensitive. Consequently, the observation of a non-SM Higgs boson at the Tevatron or the LHC would point to a rather narrow, well-defined region of MSSM parameter space [137,188] or to something beyond the minimal flavor violation framework.

Another indirect constraint on the Higgs sector comes from the search for dark matter. If dark matter particles are weakly interacting and massive, then particle physics can provide models which predict the correct relic density of the universe. In particular, the lightest supersymmetric particle, typically the lightest neutralino, is an excellent dark matter particle candidate [189]. Within the MSSM, the measured relic density places constraints in the parameter space, which in turn have implications for Higgs searches at colliders, and also for experiments looking for direct evidence of dark matter particles in elastic scattering with atomic nuclei. Large values of $\tan\beta$ and small m_A are relevant for the $b\bar{b}A/H$ and $A/H \rightarrow \tau^+\tau^-$ searches at the Tevatron, and also provide a significant contribution from the CP -even Higgs H exchange to the spin-independent cross sections for direct detection experiments such as CDMS. Consequently, a positive signal at

the Tevatron would raise prospects for a signal at CDMS, and vice-versa [187,188,190–192]. However, there are theoretical uncertainties in the calculation of dark matter scattering cross sections, and in the precise value of the local dark matter density, which are important.

IV. Charged Higgs Bosons

Charged Higgs bosons are predicted by models with an extended Higgs sector, for example, models with two Higgs field doublets (2HDM). The Higgs sector of the MSSM is a special Type-II 2HDM in which the mass of the charged Higgs boson is strongly correlated with the other Higgs boson masses. The charged Higgs boson mass in the MSSM is restricted at tree level by $m_{H^\pm} > M_W$. This restriction does not hold for some regions of parameter space after including radiative corrections. Due to the correlations among Higgs boson masses in the MSSM, the results of searches for charged Higgs bosons from LEP and the Tevatron do not significantly constrain the MSSM parameter space beyond what is already obtained from the searches for neutral Higgs bosons.

In e^+e^- collisions, charged Higgs bosons would be pair-produced via s -channel exchange of a photon or a Z boson [193]. In the 2HDM framework, the couplings are specified by the electric charge and the weak mixing angle θ_W , and the cross section at tree level depends only on the mass m_{H^\pm} . Charged Higgs bosons decay preferentially to heavy particles, but the branching ratios are model-dependent. In the Type-II 2HDM and for masses which are accessible at LEP energies, the decays $H^\pm \rightarrow c\bar{s}$ and $\tau^+\nu$ dominate. The final states $H^+H^- \rightarrow (c\bar{s})(\bar{c}s)$, $(\tau^+\nu_\tau)(\tau^-\bar{\nu}_\tau)$, and $(c\bar{s})(\tau^-\bar{\nu}_\tau) + (\bar{c}s)(\tau^+\nu_\tau)$ were considered, and the search results are usually presented as a function of $\text{BR}(H^+ \rightarrow \tau^+\nu)$. The sensitivity of the LEP searches was limited to $m_{H^\pm} < 90$ GeV, due to the background from $e^+e^- \rightarrow W^+W^-$ [194], and the kinematic limitation on the production cross section. The combined LEP data constrain $m_{H^\pm} > 78.6$ GeV independently of $\text{BR}(H^+ \rightarrow \tau^+\nu)$ [195]. The excluded limits, translated to the $(\tan\beta, m_{H^\pm})$ plane using tree level calculations of Type-II 2HDM, are shown in Fig. 13.

In the Type-I 2HDM, and if the CP -odd neutral Higgs boson A is light (which is not excluded in the general 2HDM case), the decay $H^\pm \rightarrow W^{\pm*}A$ may be dominant for masses accessible at LEP [196], a possibility that was investigated by the DELPHI collaboration [197].

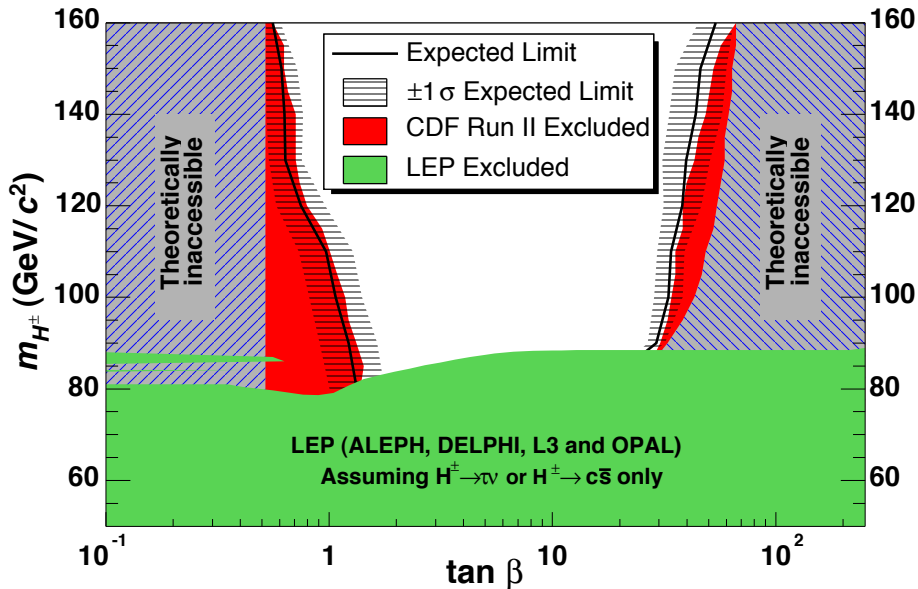


Figure 13: Summary of the 95% C.L. exclusions in the $(m_{H^\pm}, \tan \beta)$ plane obtained by LEP [195] and CDF [214]. The benchmark scenario parameters used to interpret the CDF results are very close to those of the m_h^{\max} scenario, and m_t is assumed to be 175 GeV. The full lines indicate the median limits expected in the absence of a H^\pm signal, and the horizontal hatching represents the $\pm 1\sigma$ bands about this expectation. Color version at end of book.

At hadron colliders, charged Higgs bosons can be produced in different modes. If $m_{H^\pm} < m_t - m_b$, the charged Higgs can be produced in the decays of the top quark via the decay $t \rightarrow bH^\pm$, which would compete with the SM process $t \rightarrow bW^+$. Relevant QCD and SUSY-QCD corrections to $\text{BR}(t \rightarrow H^\pm b)$ have been computed [198–201]. For $m_{H^\pm} < m_t - m_b$, the

total cross section for charged Higgs boson production (in the narrow-width approximation) is given by ³

$$\sigma(p\bar{p} \rightarrow H^\pm + X) = (1 - [\text{BR}(t \rightarrow bW^+)]^2) \sigma(p\bar{p} \rightarrow t\bar{t} + X).$$

In general, in the Type-II 2HDM, the H^+ may be observed in the decay $t \rightarrow bH^+$ at the Tevatron or at the LHC for $\tan\beta \lesssim 1$ or $\tan\beta \gg 1$.

If $m_{H^\pm} > m_t - m_b$, then charged Higgs boson production occurs mainly through radiation off a third generation quark. Single charged Higgs associated production proceeds via the $2 \rightarrow 3$ partonic processes $gg, q\bar{q} \rightarrow t\bar{b}H^-$ (and the charge conjugate final state). For charged Higgs boson production cross sections at the Tevatron and the LHC see [102,202–208].

Charged Higgs bosons can also be produced via associated production with W^\pm bosons through $b\bar{b}$ annihilation and gg -fusion [209]. They can also be produced in pairs via $q\bar{q}$ annihilation [210]. The inclusive H^+H^- cross section is less than the cross section for single charged Higgs associated production [210–212].

At the Tevatron, earlier searches by the DØ and CDF collaborations are reported in [213], and more recent searches are presented in [214,215]. Fig. 13 shows the regions excluded by the CDF search, along with the regions excluded by the LEP searches, in the MSSM for a choice of parameters which is almost identical to the m_h -max benchmark scenario adopted by the LEP collaborations in their search for neutral MSSM Higgs bosons.

Indirect limits in the $(m_{H^\pm}, \tan\beta)$ plane have been obtained by comparing the measured rate of $b \rightarrow s\gamma$ to the SM prediction. In the Type-II 2HDM and in the absence of other sources of new physics at the electroweak scale, a bound $m_{H^\pm} > 295$ GeV has been derived [177]. Although this indirect bound appears much stronger than the results from direct searches, it can be invalidated by new physics contributions, such as those which can be present in the MSSM.

³ For values of m_{H^\pm} near m_t , the width effects are important. In addition, the full $2 \rightarrow 3$ processes $p\bar{p} \rightarrow H^+\bar{t}b + X$ and $p\bar{p} \rightarrow H^-\bar{t}b + X$ must be considered.

Doubly-Charged Higgs Bosons

Higgs bosons with double electric charge are predicted, for example, by models with additional triplet scalar fields or left-right symmetric models [216]. It has been emphasized that the see-saw mechanism could lead to doubly-charged Higgs bosons with masses which are accessible to current and future colliders [217]. Searches were performed at LEP for the pair-production process $e^+e^- \rightarrow H^{++}H^{--}$ with four prompt leptons in the final state [218–220]. Lower mass bounds between 95 GeV and 100 GeV were obtained for left-right symmetric models (the exact limits depend on the lepton flavors). Doubly-charged Higgs bosons were also searched for in single production [221]. Furthermore, such particles would modify the Bhabha scattering cross section and forward-backward asymmetry via t -channel exchange. The absence of a significant deviation from the SM prediction puts constraints on the Yukawa coupling of $H^{\pm\pm}$ to electrons for Higgs boson masses which reach into the TeV range [220,221].

Searches have also been carried out at the Tevatron for the pair production process $p\bar{p} \rightarrow H^{++}H^{--}$. The DØ search is performed in the $\mu^+\mu^+\mu^-\mu^-$ final state [222], while CDF also considers $e^+e^+e^-e^-$ and $e^+\mu^+e^-\mu^-$, and final states with τ leptons [223]. Lower bounds are obtained for left- and right-handed $H^{\pm\pm}$ bosons. For example, assuming $\text{BR}(H^{\pm\pm} \rightarrow \mu^\pm\mu^\pm) = 100\%$, the DØ (CDF) data exclude a left- and a right-chiral doubly-charged Higgs boson with mass larger than 150 (136) GeV and 127 (113) GeV, respectively, at 95% C.L. A search of CDF for a long-lived $H^{\pm\pm}$ boson, which would decay outside the detector, is described in [224]. The current status of the mass and coupling limits, from direct searches at LEP and at the Tevatron, is summarized in Fig. 14.

V. Other Model Extensions

There are many ways to extend the minimal Higgs sector of the Standard Model. In the preceding sections we have considered the phenomenology of the MSSM Higgs sector, which at tree level is a constrained Type-II 2HDM (with restrictions on the Higgs boson masses and couplings), and also

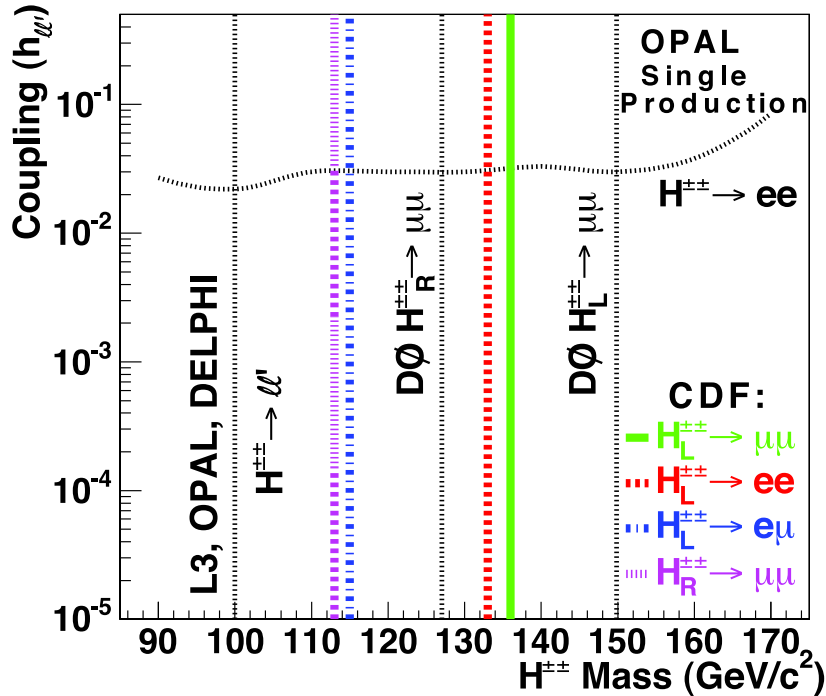


Figure 14: The 95% C.L. exclusion limits on the masses and couplings to leptons of right- and left-handed doubly-charged Higgs bosons, obtained by LEP and Tevatron experiments (from Ref. 223). Color version at end of book.

more general 2HDMs of Types I and II. Other extensions of the Higgs sector can include multiple copies of $SU(2)_L$ doublets, additional Higgs singlets, triplets or more complicated combinations of Higgs multiplets. It is also possible to enlarge the gauge symmetry beyond $SU(2)_L \times U(1)_Y$ along with the necessary Higgs structure to generate gauge boson and fermion masses. There are two main experimental constraints that govern these extensions: (*i*) precision measurements, which constrain $\rho = m_W^2 / (m_Z^2 \cos^2 \theta_W)$ to be very close to 1. In electroweak models based on the SM gauge group, the tree-level value of ρ is determined by the Higgs multiplet structure. By suitable choices for the hypercharges, and in some cases the mass splitting between the charged and neutral Higgs sector or the vacuum expectation values of the Higgs fields, it is possible to obtain a richer combination of singlets, doublets, triplets and

higher multiplets compatible with precision measurements [225]; (ii) the second important constraint comes from flavor changing neutral current (FCNC) effects. In the presence of multiple Higgs doublets, the Glashow-Weinberg theorem [226] states that tree-level FCNC's mediated by neutral Higgs bosons will be absent if all fermions of a given electric charge couple to no more than one Higgs doublet. The Higgs doublet models Type-I and Type-II are two different ways of satisfying this theorem. The coupling pattern of these two types can be arranged by imposing either a discrete symmetry or, in the case of Type-II, supersymmetry. The resulting phenomenology of extended Higgs sectors can differ significantly from that of the SM Higgs boson.

The most studied extension of the MSSM has a scalar singlet and its supersymmetric partner [227–229]. These models have an extended Higgs sector with two additional neutral scalar states (one CP -even and one CP -odd), beyond those present in the MSSM. In these models, the tree-level bound on the lightest Higgs boson, considering arguments of perturbativity of the theory up to the GUT scale, is about 100 GeV. The radiative corrections to the masses are similar to those in the MSSM, and yield an upper bound of about 145 GeV for the mass of the lightest neutral CP -even scalar [230,231]. The precise LEP II bounds on the Higgs boson masses depend on the couplings of the Higgs bosons to the gauge bosons and such couplings tend to be weakened somewhat from mixing with the singlet. The DELPHI Collaboration places constraints on such models [232], as does DØ [233].

Another extension of the MSSM which can raise the value of the lightest Higgs boson mass to a few hundred GeV is based on gauge extensions of the MSSM [234,237]. The addition of asymptotically-free gauge interactions naturally yields extra contributions to the quartic Higgs couplings. These extended gauge sector models can be combined with the presence of extra singlets or replace the singlet with a pair of triplets [236].

It is also possible that the MSSM is the low energy effective field theory of a more fundamental SUSY theory that includes additional particles with masses at or somewhat above the TeV

range, and that couple significantly to the MSSM Higgs sector. A model-independent analysis of the spectrum and couplings of the MSSM Higgs fields, based on an effective theory of the MSSM degrees of freedom has been studied in the literature [237–240]. In these scenarios the tree-level mass of the lightest CP-even state can easily be above the LEP bound of 114 GeV, thus allowing for a relatively light spectrum of superpartners, restricted only by direct searches. The Higgs spectrum and couplings can be significantly modified compared to the MSSM ones, often allowing for interesting new decay modes. It is also possible to moderately enhance the gluon fusion production cross section of the SM-like Higgs with respect to both the Standard Model and the MSSM.

Many non-SUSY solutions to the problem of electroweak symmetry breaking and the hierarchy problem are being developed. For example, the so-called “Little Higgs” models propose additional sets of heavy vector-like quarks, gauge bosons, and scalar particles, with masses in the 100 GeV to a few TeV range. The couplings of the new particles are tuned in such a way that the quadratic divergences induced in the SM by the top, gauge-boson and Higgs loops are canceled at the one-loop level. If the Little Higgs mechanism successfully resolves the hierarchy problem, it should be possible to detect some of these new states at the LHC. For reviews of models and phenomenology, and a more complete list of references, see Refs. [241] and [242].

In Little Higgs models the production and decays of the Higgs boson are modified. For example, when the dominant production mode of the Higgs is through gluon fusion, the contribution of new fermions in the loop diagrams involved in the effective ϕgg vertex can reduce the production rate. The rate is generally suppressed relative to the SM rate due to the symmetries which protect the Higgs boson mass from quadratic divergences at the one-loop level. However, the branching ratio of the Higgs to photon pairs can be enhanced in these models [243]. By design, Little Higgs models are valid only up to a scale $\Lambda \sim 5\text{--}10$ TeV. The new physics which would enter above Λ remains unspecified, and will impact the Higgs sector.

In general, it can modify Higgs couplings to third-generation fermions and gauge bosons, though these modifications are suppressed by $1/\Lambda$ [244].

Distinctive features in the Higgs phenomenology of Little Higgs models may also stem from the fact that loop-level electroweak precision bounds on models with a tree-level custodial symmetry allows for a Higgs boson heavier than the one permitted by precision electroweak fits in the SM. This looser bound follows from a cancellation of the effects on the ρ parameter of a higher mass Higgs boson and the heavy partner of the top quark. The Higgs boson can have a mass as high as 800-1000 GeV in some Little Higgs models and still be consistent with electroweak precision data [245]. Lastly, the scalar content of a Little Higgs structure is model dependent. There could be two, or even more scalar doublets in a little Higgs model, or even different representations of the electroweak gauge group [246].

Models of extra space dimensions present an alternative way of avoiding the scale hierarchy problem [14]. New states, known as Kaluza-Klein (KK) excitations, can appear at the TeV scale, where gravity-mediated interactions may become relevant. They share the quantum numbers of the graviton and/or SM particles. In a particular realization of these models, based on warped extra dimensions, a light Higgs-like particle, the radion, may appear in the spectrum [247]. The mass of the radion, as well as its possible mixing with the light Higgs boson, depends strongly on the mechanism that stabilizes the extra dimension, and on the curvature-Higgs mixing.

The radion couples to the trace of the energy-momentum tensor of the SM particles, leading to effective interactions with quarks, leptons, and weak gauge bosons which are similar to the ones of the Higgs boson, although they are suppressed by the ratio of the weak scale to the characteristic mass of the new excitations. An important characteristic of the radion is its enhanced couplings to gluons. Therefore, if it is light and mixes with the Higgs boson, it may modify the standard Higgs phenomenology at lepton and hadron colliders. A search for the radion in LEP data, conducted by OPAL using both b -tagged and flavor-independent searches, gave negative

results [248]. Radion masses below 58 GeV are excluded for the mass eigenstate which becomes the Higgs boson in the no-mixing limit, for all parameters of the Randall-Sundrum model.

In models of warped extra dimensions in which the SM particles propagate in the extra dimensions, the KK excitations of the vector-like fermions may be pair-produced at colliders and decay into combinations of two Higgs bosons and jets, or one Higgs boson, a gauge boson, and jets. KK excitations may also be singly-produced. Some of these interesting possible new signatures for SM-like Higgs bosons in association with top or bottom quarks have been studied [15].

If Higgs bosons are not discovered at the Tevatron or the LHC, other studies might be able to test alternative theories of dynamical electroweak symmetry breaking which do not involve a fundamental Higgs scalar [249].

VI. Other Searches for Higgs Bosons Beyond the SM

Decays of Higgs bosons into invisible (weakly-interacting and neutral) particles may occur in many models. For example, in the MSSM the Higgs can decay into pairs of neutralinos. In a different context, Higgs bosons might also decay into pairs of Goldstone bosons or Majorons [250]. In the process $e^+e^- \rightarrow hZ$, the mass of the invisible Higgs boson can be inferred from the kinematics of the reconstructed Z boson by using the beam energy constraint. Results from the LEP experiments can be found in Refs. [54,251]. A preliminary combination of LEP data yields a 95% C.L. lower bound of 114.4 GeV for the mass of a Higgs boson, if it is produced with SM production rate, and if it decays exclusively into invisible final states [252].

Hidden-valley models [253] predict a rich phenomenology of new particles, some of which can be long-lived and hadronize with SM particles to form exotic particles which decay at measurable distances in collider experiments. DØ has searched for pair-produced long-lived particles produced resonantly and which decay to $b\bar{b}$ pairs, and sets limits on Higgs boson production in hidden-valley models [254].

Most of the searches for the processes $e^+e^- \rightarrow hZ$ and hA , which have been discussed in the context of the *CPC*-MSSM, rely on the assumption that the Higgs bosons have a sizable branching ratio to $b\bar{b}$. However, for specific parameters of the MSSM [255], the general 2HDM case, or composite models [115,117,256], decays to non- $b\bar{b}$ final states may be significantly enhanced. Some flavor-independent searches have been reported at LEP which do not require the experimental signature of a b -jet [257], and a preliminary combination of LEP data has been performed [18,258]. If Higgs bosons are produced at the SM rate and decay only to jets of hadrons, then the 95% C.L. lower limit on the mass of the Higgs boson is 112.9 GeV, independent of the fractions of gluons and b , c , s , u and d -quarks in Higgs boson decay. In conjunction with b -flavor sensitive searches, large domains of the general Type-II 2HDM parameter space have been excluded [259].

Photonic final states from the processes $e^+e^- \rightarrow Z/\gamma^* \rightarrow H\gamma$ and from $H \rightarrow \gamma\gamma$, do not occur in the SM at tree level, but these they may proceed due to W^\pm and top quark loops [260]. Additional loops from SUSY particles would modify the rates only slightly [261], but models with anomalous couplings predict enhancements by orders of magnitude. Searches for the processes $e^+e^- \rightarrow (H \rightarrow b\bar{b})\gamma$, $(H \rightarrow \gamma\gamma)q\bar{q}$, and $(H \rightarrow \gamma\gamma)\gamma$ have been used to set limits on such anomalous couplings. These searches also contribute in the combinations of searches for the standard model Higgs boson, although the small predicted signal rates imply that they contribute less than other channels. These searches also constrain the Type-I “fermiophobic” 2HDM [262], which also predicts an enhanced $h \rightarrow \gamma\gamma$ rate. The LEP searches are described in [263,264]. In a preliminary combination of LEP data [265], a fermiophobic Higgs boson with mass less than 108.2 GeV (95% C.L.) has been excluded. Limits of about 80 GeV have been obtained at the Tevatron in Run I [266]. Run II results based on 2.7 fb^{-1} of DØ data and 3.0 fb^{-1} of CDF data extend the exclusion to 106 GeV [267]. CDF has updated this analysis with 5.4 fb^{-1} of data [268]. Other production of fermiophobic Higgs bosons, leading to a 3-photons final state, have also been searched for [269]. The Type-I 2HDM

also predicts an enhanced rate for the decays $h \rightarrow W^*W$ and Z^*Z , a possibility that has been addressed by L3 [264] and ALEPH [270].

The DELPHI collaboration has used the LEP 1 and LEP 2 data to search for Higgs bosons produced in pairs, in association with Z bosons, and in association with b quarks, and τ leptons. The decays considered are $\phi \rightarrow b\bar{b}, \tau^+\tau^-$, and to pairs of Higgs bosons, yielding four- b , four- $b+jets$, six- b and four- τ final states. No evidence for a Higgs boson was found [135], and DELPHI sets mass-dependent limits on a variety of processes, which apply to a large class of models. The limits on the cross sections of Yukawa production of Higgs bosons are typically more than 100 times larger than the SM predictions, while Higgs-strahlung limits for b and τ decays extend up to the kinematic limits of approximately 114 GeV. Limits on pair-produced Higgs bosons extend up to approximately $m_h + m_A = 140$ GeV for full-strength production, assuming $b\bar{b}$ and $\tau^+\tau^-$ decays.

OPAL's decay-mode independent search for $e^+e^- \rightarrow S^0 Z$ [53] provides sensitivity to arbitrarily-decaying scalar particles, as only the recoiling Z boson is required to be reconstructed. The energy and momentum constraints provided by the e^+e^- collisions allow the S^0 's four-vector to be reconstructed and limits placed on its production independent of its decay characteristics, allowing sensitivity for very light scalar masses. The limits obtained in this search are less than one-tenth of the SM Higgs-strahlung production rate for $1 \text{ KeV} < m_{S^0} < 19 \text{ GeV}$, and less than the SM Higgs-strahlung rate for $m_{S^0} < 81 \text{ GeV}$.

VII. Outlook

At the Tevatron, Higgs boson searches performed in several channels with 2.0 to 5.4 fb^{-1} have achieved the necessary sensitivity to test for the presence of a SM Higgs boson with a mass near $2M_W$. With anticipated improvements in analysis sensitivity, the expected total analyzed integrated luminosity of about 10 fb^{-1} , and the combination of results from both experiments, the Tevatron should be able to exclude most of the SM Higgs boson mass range up to 185 GeV (at 95% C.L.), and could produce 3σ evidence for a Higgs boson with

a mass close to 115 GeV or 160 GeV. The Tevatron searches are also sensitive to the neutral Higgs bosons of the MSSM for $m_A < 300$ GeV and $\tan \beta > 30$.

The LHC is planned to deliver proton-proton collisions at a center of mass energy of 7 TeV in 2010 and 2011, and it will produce a large data sample at the center of mass energy of 14 TeV starting in 2013. The ATLAS and CMS detectors have been optimized for Higgs boson searches. The discovery of a SM Higgs boson is expected to be possible over the mass range between 100 GeV and 1 TeV, given sufficient integrated luminosity. This broad range is covered by a variety of searches based on several production and decay processes. The LHC experiments are expected to provide full coverage of the MSSM parameter space by direct searches for the h , H , A , and H^\pm bosons, and by searching for h bosons in cascade decays of SUSY particles. The simultaneous discovery of several of the Higgs bosons is expected to be possible over extended domains of the MSSM parameter space.

A high-energy e^+e^- linear collider may start operation around the year 2020. According to present planning, it would run initially at a center-of-mass energy of 500 GeV, and an upgrade would allow running at 1 TeV later [22]. One of the primary goals is to extend precision measurements, which are typical of e^+e^- colliders, to the Higgs sector. According to several studies, the Higgs couplings to fermions and vector bosons could be measured with a precision of a few percent, and the parameters of the MSSM could be studied in great detail. At the highest collider energies and luminosities, the self-coupling of the Higgs fields could be measured directly through final states with two Higgs bosons [271].

Higgs boson production in the s -channel might be possible at a future $\mu^+\mu^-$ collider [23]. Mass measurements with a precision of a few MeV would be possible, and the total width could be obtained directly from Breit-Wigner scans. The heavy CP -even and CP -odd bosons, H and A , degenerate over most of the MSSM parameter space, could be directly disentangled from the line shape.

Higgs bosons enter calculations of electroweak observables through loop effects, so it has been possible to constrain the SM Higgs sector using a global fit to precision electroweak measurements. The fit favors Higgs bosons that are not heavy, a fact which is compatible with the predictions of the MSSM. B -physics observables explored at CLEO, BaBar, Belle and the Tevatron independently constrain the MSSM parameter space available for Higgs searches. These indirect limits derive in part from the specific effects on flavor physics of the supersymmetry-breaking mechanism. The combined information of direct and indirect SUSY Higgs searches together with the results from direct search for dark matter, could provide important information about supersymmetry.

In the theoretical landscape, several models are emerging with novel approaches to the problem of electroweak symmetry breaking. Many of them incorporate a Higgs sector with features distinctly different from the SM, and their phenomenology could be studied at the LHC.

There is uncertainty on the mass range for the scale of new physics. It arises from one side by the attempt to explain the hierarchy between the electroweak scale and the Planck scale in a natural way, which demands new physics at or below the TeV scale, and on the other side by the strong bounds at that same scale, of order of a TeV or larger, that come from the precise measurements delivered by the experiments in the last two decades. Supersymmetry remains a suggestive candidate for new physics. Models with no fundamental Higgs bosons are harder to accommodate with precision data, but the LHC and a future lepton collider will be able to make strong statements about the mechanism of electroweak symmetry breaking.

References

1. P.W. Higgs, Phys. Rev. Lett. **12**, 132 (1964);
idem, Phys. Rev. **145**, 1156 (1966);
 F. Englert and R. Brout, Phys. Rev. Lett. **13**, 321 (1964);
 G.S. Guralnik, C.R. Hagen, and T.W. Kibble, Phys. Rev. Lett. **13**, 585 (1964).
2. S.L. Glashow, Nucl. Phys. **20**, 579 (1961);
 S. Weinberg, Phys. Rev. Lett. **19**, 1264 (1967);

- A. Salam, *Elementary Particle Theory*, eds.: Svartholm, Almquist, and Wiksell, Stockholm, 1968;
 S. Glashow, J. Iliopoulos, and L. Maiani, Phys. Rev. **D2**, 1285 (1970).
3. J.M. Cornwall, D.N. Levin, and G. Tiktopoulos, Phys. Rev. Lett. **30**, 1286 (1973); Phys. Rev. **D10**, 1145 (1974).;
 C.H. Llewellyn Smith, Phys. Lett. **B46**, 233 (1973).
 4. B.W. Lee, C. Quigg, and H.B. Thacker, Phys. Rev. **D16**, 1519 (1977).
 5. LEP Electroweak Working Group, status of August 2009, <http://lepewwg.web.cern.ch/LEPEWWG/>;
 The ALEPH, CDF, DØ, DELPHI, L3, OPAL, SLD Collabor., the LEP Electroweak Working Group, the Tevatron Electroweak Working Group, and the SLD Electroweak and Heavy Flavor groups, LEPEWWG/2009-01 (2009);
 J. Erler and P. Langacker, *Electroweak Model and Constraints on New Physics*, in this volume.
 6. M. Bona *et al.*, [UTfit Collab.], arXiv:0908.3470 [hep-ph]; http://ckmfitter.in2p3.fr/plots_Moriond09.
 7. J. Wess and B. Zumino, Nucl. Phys. **B70**, 39 (1974);
 idem., Phys. Lett. **49B**, 52 (1974);
 H.P. Nilles, Phys. Rev. **C110**, 1 (1984);
 H.E. Haber and G.L. Kane, Phys. Rev. **C117**, 75 (1985);
 S.P. Martin, arXiv:hep-ph/9709356 (1997);
 P. Fayet, Phys. Lett. **B69**, 489 (1977);
 ibid., **B84**, 421 (1979);
 ibid., **B86**, 272 (1979);
 idem., Nucl. Phys. **B101**, 81 (2001).
 8. J.F. Gunion *et al.*, *The Higgs Hunter’s Guide* (Addison-Wesley) 1990;
 A. Djouadi, arXiv:hep-ph/0503172 (2005),
 arXiv:hep-ph/0503173 (2005).
 9. A detailed discussion and list of references is given in subsection III.
 10. L.E. Ibáñez and G.G. Ross, Phys. Lett. **B105**, 439 (1981);
 S. Dimopoulos, S. Raby, and F. Wilczek, Phys. Rev. **D24**, 1681 (1981);
 M.B. Einhorn and D.R.T. Jones, Nucl. Phys. **B196**, 475 (1982);
 W.J. Marciano and G. Senjanovic, Phys. Rev. **D25**, 3092 (1982).

11. J. Ellis, S. Kelley, and D.V. Nanopoulos, Phys. Lett. **B249**, 441 (1990);
 P. Langacker and M. Luo, Phys. Rev. **D44**, 817 (1991);
 U. Amaldi, W. de Boer, and H. Fürstenau, Phys. Lett. **B260**, 447 (1991);
 P. Langacker and N. Polonsky, Phys. Rev. **D52**, 3081 (1995);
 S. Pokorski, *Act. Phys. Pol.* **B30**, 1759 (1999);
 For a recent review, see: R.N. Mohapatra, in *Particle Physics 1999, Proceedings of the ICTP Summer School in Particle Physics*, Trieste, Italy, 21 June–9 July, 1999, eds. G. Senjanovic and A.Yu. Smirnov. (World Scientific, Singapore, 2000) pp. 336–394.
12. S. Weinberg, Phys. Rev. **D13**, 974 (1979); Phys. Rev. **D19**, 1277 (1979);
 L. Susskind, Phys. Rev. **D20**, 2619 (1979);
 E. Farhi and L. Susskind, Phys. Rev. **74**, 277 (1981);
 R.K. Kaul, Rev. Mod. Phys. **55**, 449 (1983);
 C.T. Hill and E.H. Simmons, Phys. Reports **381**, 235 (2003) [E: *ibid.*, **390**, 553 (2004)].
13. N. Arkani-Hamed, A.G. Cohen, and H. Georgi, Phys. Lett. **B513**, 232 (2001);
 N. Arkani-Hamed *et al.*, JHEP **0207**, 034 (2002);
 N. Arkani-Hamed *et al.*, JHEP **0208**, 020 (2002);
 N. Arkani-Hamed *et al.*, JHEP **0208**, 021 (2002);
 I. Low, W. Skiba, and D. Smith, Phys. Rev. **D66**, 072001 (2002).
14. I. Antoniadis, Phys. Lett. **B246**, 377 (1990);
 N. Arkani-Hamed, S. Dimopoulos, and G.R. Dvali, Phys. Lett. **B429**, 263 (1998);
 L. Randall and R. Sundrum, Phys. Rev. Lett. **83**, 3370 (1999) *idem*, **84**, 4690 (1999);
 G.F. Giudice *et al.*, Nucl. Phys. **B544**, 3 (1999);
 C. Csáki *et al.*, Phys. Rev. **D63**, 065002 (2001).
15. J. A. Aguilar-Saavedra, JHEP **0612**, 033 (2006);
 M. Carena *et al.*, Phys. Rev. **D76**, 035006 (2007);
 A.D. Medina, N.R. Shah, and C.E.M. Wagner,
[arXiv:0706.1281](https://arxiv.org/abs/0706.1281) (2007);
 A. Djouadi and G. Moreau, [arXiv:0707.3800](https://arxiv.org/abs/0707.3800) (2007);
 H. Davoudiasl, B. Lillie, and T. G. Rizzo, JHEP **0608**, 042 (2006);
 A. Falkowski, [arXiv:0711.0828](https://arxiv.org/abs/0711.0828) (2007).
16. P.J. Franzini and P. Taxil, in *Z physics at LEP 1*, CERN 89-08 (1989).

17. ALEPH, DELPHI, L3, and OPAL Collabs., The LEP Working Group for Higgs Boson Searches, Phys. Lett. **B565**, 61 (2003).
18. ALEPH, DELPHI, L3, and OPAL Collabs., The LEP Working Group for Higgs Boson Searches, Eur. Phys. J. **C47**, 547 (2006).
19. The CDF and DØ Collabs., Phys. Rev. Lett. **104**, 061802 (2010).
20. ATLAS Collab., arXiv:0901.0512 [hep-ex].
21. CMS Collab., J. Phys. **G34**, 995 (2007).
22. E. Accomando *et al.*, Physics Reports **299**, 1–78 (1998); TESLA Technical Design Report, Part 3: *Physics at an e^+e^- Linear Collider*, arXiv:hep-ph/0106315 (2001); ACFA Linear Collider Working Group, *Particle Physics Experiments at JLC*, arXiv:hep-ph/0109166 (2001); A. Djouadi *et al.*, *ILC Global Design Effort and World Wide Study*, arXiv:0709.1893 [hep-ph] (2007); E. Accomando *et al.*, CLIC Physics Working Group, arXiv:hep-ph/0412251 (2004); J. Brau *et al.*, [ILC Collab.], arXiv:0712.1950 [physics.acc-ph] (2007); G. Aarons *et al.*, [ILC Collab.], arXiv:0709.1893 [hep-ph] (2007).
23. B. Autin *et al.*, (eds.), CERN 99-02; C.M. Ankenbrandt *et al.*, Phys. Rev. ST Acc. Beams **2**, 081001 (1999); C. Blochinger *et al.*, *Physics Opportunities at $\mu^+\mu^-$ Higgs Factories*, arXiv:hep-ph/0202199 (2002).
24. T. van Ritbergen and R. G. Stuart, Phys. Rev. Lett. **82**, 488 (1999); T. van Ritbergen and R. G. Stuart, Nucl. Phys. **B564**, 343 (2000); M. Steinhauser and T. Seidensticker, Phys. Lett. **B467**, 271 (1999).
25. N. Cabibbo *et al.*, Nucl. Phys. **B158**, 295 (1979); See, *e.g.*, G. Altarelli and G. Isidori, Phys. Lett. **B337**, 141 (1994); J.A. Casas, J.R. Espinosa, and M. Quirós, Phys. Lett. **B342**, 171 (1995) *idem.*, Phys. Lett. **B382**, 374 (1996); T. Hambye and K. Riesselmann, Phys. Rev. **D55**, 7255 (1997).
26. J. R. Espinosa and M. Quiros, Phys. Lett. **B353**, 257 (1995); G. Isidori *et al.*, Nucl. Phys. **B609**, 387 (2001).

27. B.A. Kniehl, Phys. Rept. **240**, 211 (1994).
28. E. Gross *et al.*, Z. Phys. **C63**, 417 (1994); [E: *ibid.*, **C66**, 32 (1995)];
 E. Braaten and J.P. Leveille, Phys. Rev. **D22**, 715 (1980);
 N. Sakai, Phys. Rev. **D22**, 2220 (1980);
 T. Inami and T. Kubota, Nucl. Phys. **B179**, 171 (1981);
 S.G. Gorishniĭ, A.L. Kataev, and S.A. Larin, Sov. J. Nucl. Phys. **40**, 329 (1984) [*Yad. Fiz.* **40**, 517 (1984)];
 M. Drees and K. Hikasa, Phys. Lett. **B240**, 455 (1990) [E: **B262**, 497 (1991)];
 A. Djouadi, M. Spira, and P.M. Zerwas, Z. Phys. **C70**, 675 (1996);
 A. Djouadi, J. Kalinowski, and M. Spira, Comput. Phys. Commun. **108**, 56 (1998);
 B.A. Kniehl, Nucl. Phys. **B376**, 3 (1992);
 A.L. Kataev, Sov. Phys. JETP Lett. **66**, 327 (1997) [*Pis'ma Zh. Éksp. Teor. Fiz.* **66**, 308 (1997)].
29. For a compilation of theoretical results for SM and MSSM Higgs cross sections at the Tevatron and the LHC see:
<http://maltoni.home.cern.ch/maltoni/TeV4LHC/>.
 The text of this review describes recent updates.
30. R.V. Harlander and W.B. Kilgore, Phys. Rev. Lett. **88**, 201801 (2002);
 C. Anastasiou and K. Melnikov, Nucl. Phys. **B646**, 220 (2002);
 V. Ravindran, J. Smith, and W.L. van Neerven, Nucl. Phys. **B665**, 325 (2003);
 M. Spira *et al.*, Nucl. Phys. **B453**, 17 (1995).
31. S. Actis *et al.*, Phys. Lett. **B670**, 12 (2008);
 U. Aglietti *et al.*, Phys. Lett. **B595**, 432 (2004);
 G. Degrassi and F. Maltoni, Phys. Lett. **B600**, 255 (2004).
32. C. Anastasiou, R. Boughezal, and F. Petriello, JHEP **0904**, 003 (2009).
33. S. Catani *et al.*, JHEP **0307**, 028 (2003);
 S. Moch and A. Vogt, Phys. Lett. **B631**, 48 (2005);
 E. Laenen and L. Magnea, Phys. Lett. **B632**, 270 (2006);
 A. Idilbi *et al.*, Phys. Rev. **D73**, 077501 (2006).
34. D. de Florian and M. Grazzini, Phys. Lett. **B674**, 291 (2009).
35. V. Ahrens *et al.*, Eur. Phys. J. **C62**, 333 (2009).
36. C.R. Schmidt, Phys. Lett. **B413**, 391 (1997).

37. D. de Florian, M. Grazzini, and Z. Kunszt, Phys. Rev. Lett. **82**, 5209 (1999).
38. Nucl. Phys. **B634**, 247 (2002).
39. C.J. Glosser and C.R. Schmidt, JHEP **0212**, 016 (2002).
40. J.M. Campbell, R.K. Ellis, and G. Zanderighi, JHEP **0610**, 028 (2006).
41. J.M. Campbell, R.K. Ellis, and C. Williams, arXiv:1001.4495 [hep-ph].
42. K.A. Assamagan *et al.*, arXiv:hep-ph/0406152 (2004).
43. O. Brein, A. Djouadi, and R. Harlander, Phys. Lett. **B579**, 149 (2004);
M.L. Ciccolini, S. Dittmaier, and M. Krämer, Phys. Rev. **D68**, 073003 (2003).
44. P. Bolzoni *et al.*, arXiv:1003.4451 [hep-ph] (2010);
T. Han, G. Valencia, and S. Willenbrock, Phys. Rev. Lett. **69**, 3274 (1992);
E.L. Berger and J. Campbell, Phys. Rev. **D70**, 073011 (2004);
T. Figy, C. Oleari, and D. Zeppenfeld, Phys. Rev. **D68**, 073005 (2003).
45. W. Beenakker *et al.*, Phys. Rev. Lett. **87**, 201805 (2001);
L. Reina and S. Dawson, Phys. Rev. Lett. **87**, 201804 (2001);
S. Dawson *et al.*, Phys. Rev. **D67**, 071503 (2003).
46. R.V. Harlander and W.B. Kilgore, Phys. Rev. **D68**, 013001 (2003);
J. Campbell *et al.*, Phys. Rev. **D67**, 095002 (2003);
S. Dawson *et al.*, Phys. Rev. Lett. **94**, 031802 (2005);
S. Dittmaier, M. Krämer, and M. Spira, Phys. Rev. **D70**, 074010 (2004);
S. Dawson *et al.*, Phys. Rev. **D69**, 074027 (2004).
47. W.J. Stirling and D.J. Summers, Phys. Lett. **B283**, 411 (1992);
F. Maltoni *et al.*, Phys. Rev. **D64**, 094023 (2001).
48. M. Carena and H.E. Haber, Prog. in Part. Nucl. Phys. **50**, 152 (2003).
49. J. Ellis *et al.*, Nucl. Phys. **B106**, 292 (1976);
B.L. Ioffe and V.A. Khoze, Sov. J. Nucl. Phys. **9**, 50 (1978).
50. D.R.T. Jones and S.T. Petcov, Phys. Lett. **84B**, 440 (1979);
R.N. Cahn and S. Dawson, Phys. Lett. **136B**, 96 (1984);
ibid., **138B**, 464 (1984);
W. Kilian *et al.*, Phys. Lett. **B373**, 135 (1996).

51. P. Janot, *Searching for Higgs Bosons at LEP 1 and LEP 2*, in Perspectives in Higgs Physics II, World Scientific, ed. G.L. Kane (1998).
52. See the Review on *Statistics* in this volume.
53. OPAL Collab., Eur. Phys. J. **C27**, 311 (2003).
54. ALEPH Collab., Phys. Lett. **B526**, 191 (2002).
55. DELPHI Collab., Eur. Phys. J. **C32**, 145 (2004).
56. L3 Collab., Phys. Lett. **B517**, 319 (2001).
57. OPAL Collab., Eur. Phys. J. **C26**, 479 (2003).
58. The CDF and DØ Collabs. and the Tevatron Electroweak Working Group, *Combination of the CDF and DØ Results on the Mass of the Top Quark*, [arXiv:0903.2503 \[hep-ex\]](https://arxiv.org/abs/0903.2503) (2009).
59. The CDF and DØ Collabs. and the Tevatron Electroweak Working Group, *Updated Combination of CDF and DØ Results for the Mass of the W Boson*, [arXiv:0908.1374 \[hep-ex\]](https://arxiv.org/abs/0908.1374) (2009);
The ALEPH, DELPHI, L3, and OPAL Collabs. and the LEP Electroweak Working Group, [arXiv:hep-ex/0612034](https://arxiv.org/abs/hep-ex/0612034) (2006).
60. S.L. Glashow, D.V. Nanopoulos, and A. Yildiz, Phys. Rev. **D18**, 1724 (1978);
A. Stange, W. Marciano, and S. Willenbrock, Phys. Rev. **D49**, 1354 (1994); *ibid.*, **D50**, 4491 (1994).
61. CDF Collab., Phys. Rev. Lett. **103**, 101802 (2009).
62. DØ Collab., Phys. Rev. Lett. **102**, 051803 (2009).
63. (**) CDF Collab., CDF Note 10068, “Search for Standard Model Higgs Boson Production in Association with W Boson Using Matrix Element Techniques with 4.8 fb^{-1} of CDF Data” (2010).
64. (***) DØ Collab., DØ Note 5972-CONF, “Search for WH associated production using neural networks with 5.0 fb^{-1} of Tevatron data” (2009).
65. CDF Collab., Phys. Rev. Lett. **104**, 141801 (2010).
66. DØ Collab., Phys. Rev. Lett. **104**, 071801 (2010).
67. (**) CDF Collab., CDF Note 9642, “Search for the Standard Model Higgs Boson in the \cancel{E}_T plus jets sample” (2009).
68. CDF Collab., Phys. Rev. **D80**, 071101 (2009).
69. DØ Collab., Phys. Lett. **B655**, 209 (2007).
70. (**) CDF Collab., CDF Note 9889, “A Search for the Standard Model Higgs Boson in the Process $ZH \rightarrow \ell^+\ell^- b\bar{b}$ Using 4.1 fb^{-1} of CDF II Data” (2009).

71. (***) DØ Collab., DØ Note 5876-CONF, “Search for $ZH(\rightarrow e^+e^-b\bar{b})$ and $ZH(\rightarrow \mu^+\mu^-b\bar{b})$ Production in 4.2 fb^{-1} of data with the DØ Detector in $p\bar{p}$ collisions at $\sqrt{s} = 1.96 \text{ TeV}$ ” (2009).
72. (**) CDF Collab., CDF Note 9248, “Search for the Standard Model Higgs Boson in the $H \rightarrow \tau^+\tau^-$ Channel at CDF Run II” (2008).
73. DØ Collab., Phys. Rev. Lett. **102**, 251801 (2009).
74. (***) DØ Collab., DØ Note 5845-CONF, “Search for the SM Higgs boson in the $\tau^+\tau^-q\bar{q}$ final state” (2009).
75. (***) DØ Collab., DØ Note 5977-CONF, “Search for the standard model Higgs boson in the $WH \rightarrow \tau\nu b\bar{b}$ channel with 4.0 fb^{-1} of $p\bar{p}$ collisions at $\sqrt{s} = 1.96 \text{ TeV}$ ” (2009).
76. (**) CDF Collab., CDF Note 9997, “Search for Standard Model Higgs Boson Production in Association with W Boson using 4.3 fb^{-1} of CDF Data” (2009);
 (**) CDF Collab., CDF Note 9985, “Search for Standard Model Higgs Boson Production in Association with W Boson Using Matrix Element Techniques with 4.3 fb^{-1} of CDF Data” (2009).
77. CDF Collab., Phys. Rev. Lett. **103**, 221801 (2009).
78. The CDF and DØ Collabs. and the Tevatron New Physics and Higgs Working Group,
[arXiv:0911.3930 \[hep-ex\]](https://arxiv.org/abs/0911.3930) (2009).
79. DØ Collab., Phys. Rev. Lett. **97**, 151804 (2006).
80. (**) CDF Collab., CDF Note 7307, “Search for the WH Production Usign High- p_T Isolated Like-Sign Dilepton Events in Run II” (2004).
81. (***) DØ Collab., DØ Note 5873-CONF, “Search for the Associated Higgs Boson Production with Like Sign Leptons in $p\bar{p}$ Collisions $\sqrt{s} = 1.96 \text{ TeV}$ ” (2009).
82. CDF Collab., Phys. Rev. Lett. **104**, 061803 (2010).
83. DØ Collab., Phys. Rev. Lett. **104**, 061804 (2010).
84. G.D. Kribs *et al.*, Phys. Rev. **D76**, 075016 (2007).
85. P. Bechtle *et al.*, Comput. Phys. Commun. **181**, 138 (2010).
86. C.J. Flacco *et al.*, [arXiv:1005.1077 \[hep-ph\]](https://arxiv.org/abs/1005.1077) (2010).
87. The CDF and DØ Collabs.,
[arXiv:1005.3216 \[hep-ex\]](https://arxiv.org/abs/1005.3216) (2010).
88. C. Anastasiou, R. Boughezal, and E. Furlan,
[arXiv:1003.4677 \[hep-ph\]](https://arxiv.org/abs/1003.4677) (2010).
89. A. Schafer, O. Nachtmann, and R. Schopf, Phys. Lett. **B249**, 331 (1990);

- A. Bialas and P.V. Landshoff, Phys. Lett. **B256**, 540 (1991);
 M. Heyssler, Z. Kunszt, and W.J. Stirling Phys. Lett. **B406**, 95 (1997);
 R. Enberg *et al.*, Phys. Rev. Lett. **89**, 081801 (2002);
 V.A. Khoze, A.D. Martin, and M.G. Ryskin, Phys. Lett. **B401**, 330 (1997); Eur. Phys. J. **C14**, 525 (2000);
 Eur. Phys. J. **C25**, 391 (2002); Eur. Phys. J. **C26**, 229 (2002);
 A.B. Kaidalov *et al.*, Eur. Phys. J. **C33**, 261 (2004);
 C. Royon, Mod. Phys. Lett. **A18**, 2169 (2003).
90. E. Yazgan *et al.*, CMS-NOTE-2007-011 and
[arXiv:0706.1898 \[hep-ex\]](https://arxiv.org/abs/0706.1898) (2007).
91. J.-J. Blaising *et al.*, “Potential LHC contributions to Europe’s future Strategy at the high energy frontier,” input number 54 to the CERN Council Strategy Group,
<http://council-strategygroup.web.cern.ch/council-strategygroup/>.
92. G. Azuelos *et al.*, Eur. Phys. J. **C66**, 525 (2010).
93. V. Buescher and K. Jakobs, Int. J. Mod. Phys. **A20**, 2523 (2005).
94. D. Zeppenfeld *et al.*, Phys. Rev. **D62**, 013009 (2000);
 D. Zeppenfeld, “Higgs Couplings at the LHC,” in *Proceedings of the APS/DPF/DPB Summer Study on the Future of Particle Physics* (Snowmass 2001), eds. R. Davidson and C. Quigg, SNOWMASS-2001-P123,
[arXiv:hep-ph/0203123](https://arxiv.org/abs/hep-ph/0203123) (2002).
95. M. Dührssen *et al.*, Phys. Rev. **D70**, 113009 (2004).
96. T. Plehn, D.L. Rainwater, and D. Zeppenfeld, Phys. Rev. Lett. **88**, 051801 (2002).
97. V. Hankele *et al.*, Phys. Rev. **D74**, 095001 (2006).
98. C. Ruwiedel, N. Wermes, and M. Schumacher, Eur. Phys. J. **C51**, 385 (2007).
99. E. Witten, Nucl. Phys. **B188**, 513 (1981);
 R.K. Kaul, Phys. Lett. **B109**, 19 (1982);
Pramana **19**, 183 (1982);
 L. Susskind, Phys. Rev. **104**, 181 (1984).
100. L.E. Ibáñez and G.G. Ross, Phys. Lett. **B110**, 215 (1982);
 L.E. Ibáñez, Phys. Lett. **B118**, 73 (1982);
 J. Ellis, D.V. Nanopoulos, and K. Tamvakis, Phys. Lett. **B121**, 123 (1983);
 L. Alvarez-Gaumé, J. Polchinski, and M.B. Wise, Nucl. Phys. **B221**, 495 (1983).

101. S. Dimopoulos and H. Georgi, Nucl. Phys. **B193**, 150 (1981);
 K. Harada and N. Sakai, Prog. Theor. Phys. **67**, 1877 (1982);
 K. Inoue *et al.*, Prog. Theor. Phys. **67**, 1889 (1982);
 L. Girardello and M.T. Grisaru, Nucl. Phys. **B194**, 65 (1982);
 L.J. Hall and L. Randall, Phys. Rev. Lett. **65**, 2939 (1990);
 I. Jack and D.R.T. Jones, Phys. Lett. **B457**, 101 (1999).
102. H.E. Haber and G.L. Kane, Phys. Rev. **C117**, 75 (1985);
 H.E. Haber, *Supersymmetry*, in this volume.
103. S. Dimopoulos and D.W. Sutter, Nucl. Phys. **B452**, 496 (1995);
 D.W. Sutter, Stanford Ph. D. thesis, hep-ph/9704390 (1997);
 H.E. Haber, Nucl. Phys. B (Proc. Suppl.) **62A-C**, 469 (1998).
104. H.E. Haber and Y. Nir, Nucl. Phys. **B335**, 363 (1990);
 A. Dobado, M.J. Herrero, and S. PenaRanda, Eur. Phys. J. **C17**, 487 (2000);
 J.F. Gunion and H.E. Haber, Phys. Rev. **D67**, 075019 (2003).
105. L.J. Hall and M.B. Wise, Nucl. Phys. **B187**, 397 (1981).
106. Y. Okada, M. Yamaguchi, and T. Yanagida, Prog. Theor. Phys. **85**, 1 (1991);
 J. Ellis, G. Ridolfi, and F. Zwirner, Phys. Lett. **B257**, 83 (1991).
107. H.E. Haber and R. Hempfling, Phys. Rev. Lett. **66**, 1815 (1991).
108. S.P. Li and M. Sher, Phys. Lett. **B140**, 339 (1984);
 R. Barbieri and M. Frigeni, Phys. Lett. **B258**, 395 (1991);
 M. Drees and M.M. Nojiri, Phys. Rev. **D45**, 2482 (1992);
 J.A. Casas *et al.*, Nucl. Phys. **B436**, 3 (1995) [E: **B439**, 466 (1995)];
 J. Ellis, G. Ridolfi, and F. Zwirner, Phys. Lett. **B262**, 477 (1991);
 A. Brignole *et al.*, Phys. Lett. **B271**, 123 (1991) [E: **B273**, 550 (1991)].
109. R.-J. Zhang, Phys. Lett. **B447**, 89 (1999);
 J.R. Espinosa and R.-J. Zhang, JHEP **0003**, 026 (2000);
 J.R. Espinosa and R.-J. Zhang, Nucl. Phys. **B586**, 3 (2000);

- A. Brignole *et al.*, Nucl. Phys. **B631**, 195 (2002), Nucl. Phys. **B643**, 79 (2002);
 A. Dedes, G. Degrassi, and P. Slavich, Nucl. Phys. **B672**, 144 (2003).
110. H.E. Haber and R. Hempfling, Phys. Rev. Lett. **66**, 1815 (1991);
 J.F. Gunion and A. Turski, Phys. Rev. **D39**, 2701 (1989), Phys. Rev. **D40**, 2333 (1989);
 M.S. Berger, Phys. Rev. **D41**, 225 (1990);
 A. Brignole, Phys. Lett. **B277**, 313 (1992); Phys. Lett. **B281**, 284 (1992);
 M.A. Díaz and H.E. Haber, Phys. Rev. **D45**, 4246 (1992);
 P.H. Chankowski, S. Pokorski, and J. Rosiek; Phys. Lett. **B274**, 191 (1992); Nucl. Phys. **B423**, 437 (1994);
 A. Yamada, Phys. Lett. **B263**, 233 (1991); Z. Phys. **C61**, 247 (1994);
 A. Dabelstein, Z. Phys. **C67**, 496 (1995);
 R. Hempfling and A.H. Hoang, Phys. Lett. **B331**, 99 (1994);
 S. Heinemeyer, W. Hollik, and G. Weiglein, Phys. Rev. **D58**, 091701 (1998); Phys. Lett. **B440**, 296 (1998); Eur. Phys. J. **C9**, 343 (1999).
111. D.M. Pierce *et al.*, Nucl. Phys. **B491**, 3 (1997).
112. R. Barbieri, M. Frigeni, and F. Caravaglios, Phys. Lett. **B258**, 167 (1991);
 Y. Okada, M. Yamaguchi, and T. Yanagida, Phys. Lett. **B262**, 45 (1991);
 J.R. Espinosa and M. Quirós, Phys. Lett. **B266**, 389 (1991);
 D.M. Pierce, A. Papadopoulos, and S. Johnson, Phys. Rev. Lett. **68**, 3678 (1992);
 K. Sasaki, M. Carena, and C.E.M. Wagner, Nucl. Phys. **B381**, 66 (1992);
 R. Hempfling, in *Phenomenological Aspects of Supersymmetry*, eds. W. Hollik, R. Rückl, and J. Wess (Springer-Verlag, Berlin, 1992) pp. 260–279;
 J. Kodaira, Y. Yasui, and K. Sasaki, Phys. Rev. **D50**, 7035 (1994);
 H.E. Haber and R. Hempfling, Phys. Rev. **D48**, 4280 (1993);
 M. Carena *et al.*, Phys. Lett. **B355**, 209 (1995);
 M. Carena, M. Quirós, and C.E.M. Wagner, Nucl. Phys. **B461**, 407 (1996).

113. H.E. Haber, R. Hempfling, and A.H. Hoang, Z. Phys. **C75**, 539 (1997);
M. Carena *et al.*, Nucl. Phys. **B580**, 29 (2000).
114. S. Martin, Phys. Rev. **D67**, 095012 (2003); Phys. Rev. **D71**, 016012 (2005); Phys. Rev. **D75**, 055005 (2007).
115. M. Carena, S. Mrenna, and C.E.M. Wagner, Phys. Rev. **D60**, 075010 (1999); *ibid.*, Phys. Rev. **D62**, 055008 (2000).
116. S. Heinemeyer, W. Hollik, and G. Weiglein, Phys. Lett. **B455**, 179 (1999);
J.R. Espinosa and I. Navarro, Nucl. Phys. **B615**, 82 (2001);
G. Degrassi, P. Slavich, and F. Zwirner, Nucl. Phys. **B611**, 403 (2001);
S. Heinemeyer *et al.*, Eur. Phys. J. **C39**, 465 (2005).
117. M. Carena *et al.*, hep-ph/9912223 (1999); *idem*, Eur. Phys. J. **C26**, 601 (2003).
118. G. Degrassi *et al.*, Eur. Phys. J. **C28**, 133 (2003).
119. S. Heinemeyer *et al.*, J. High Energy Phys. **0808**, 087 (2008).
120. M. Carena *et al.*, Phys. Lett. **B495**, 155 (2000);
M. Carena *et al.*, Nucl. Phys. **B625**, 345 (2002).
121. A. Dabelstein, Nucl. Phys. **B456**, 25 (1995);
F. Borzumati *et al.*, Nucl. Phys. **B555**, 53 (1999);
H. Eberl *et al.*, Phys. Rev. **D62**, 055006 (2000).
122. J.A. Coarasa, R.A. Jiménez, and J. Solà, Phys. Lett. **B389**, 312 (1996);
R.A. Jiménez and J. Solà, Phys. Lett. **B389**, 53 (1996);
A. Bartl *et al.*, Phys. Lett. **B378**, 167 (1996).
123. S. Heinemeyer, W. Hollik and G. Weiglein, Eur. Phys. J. **C16**, 139 (2000).
124. H.E. Haber *et al.*, Phys. Rev. **D63**, 055004 (2001).
125. L. Hall, R. Rattazzi, and U. Sarid, Phys. Rev. **D50**, 7048 (1994);
R. Hempfling, Phys. Rev. **D49**, 6168 (1994).
126. M. Carena *et al.*, Nucl. Phys. **B426**, 269 (1994).
127. M. Carena *et al.*, Phys. Lett. **B499**, 141 (2001).
128. E. Berger *et al.*, Phys. Rev. **D66**, 095001 (2002).
129. E. Boos *et al.*, Phys. Rev. **D66**, 055004 (2002).
130. A. Djouadi, J. Kalinowski, and P.M. Zerwas, Z. Phys. **C57**, 569 (1993);
H. Baer *et al.*, Phys. Rev. **D47**, 1062 (1993);
A. Djouadi *et al.*, Phys. Lett. **B376**, 220 (1996);

- A. Djouadi *et al.*, Z. Phys. **C74**, 93 (1997);
 S. Heinemeyer and W. Hollik, Nucl. Phys. **B474**, 32 (1996).
131. J.F. Gunion, Phys. Rev. Lett. **72**, 199 (1994);
 D. Choudhury and D.P. Roy, Phys. Lett. **B322**, 368 (1994);
 O.J. Eboli and D. Zeppenfeld, Phys. Lett. **B495**, 147 (2000);
 B.P. Kersevan, M. Malawski, and E. Richter-Was, Eur. Phys. J. **C29**, 541 (2003).
132. OPAL Collab., Eur. Phys. J. **C37**, 49 (2004).
133. L3 Collab., Phys. Lett. **B545**, 30 (2002).
134. OPAL Collab., Eur. Phys. J. **C23**, 397 (2002).
135. DELPHI Collab., Eur. Phys. J. **C38**, 1 (2004).
136. J.F. Gunion and H.E. Haber, Nucl. Phys. **B278**, 449 (1986) [E: **B402**, 567 (1993)];
 S. Dawson, A. Djouadi, and M. Spira, Phys. Rev. Lett. **77**, 16 (1996);
 A. Djouadi, Phys. Lett. **B435**, 101 (1998);
 A. Djouadi *et al.*, Phys. Lett. **B318**, 347 (1993);
 R.V. Harlander and W.B. Kilgore, JHEP **0210**, 017 (2002);
 C. Anastasiou and K. Melnikov, Phys. Rev. **D67**, 037501 (2003);
 J. Guasch, P. Hafliger, and M. Spira, Phys. Rev. **D68**, 115001 (2003);
 R.V. Harlander and M. Steinhauser, JHEP **0409**, 066 (2004);
 S. Dawson *et al.*, Mod. Phys. Lett. **A21**, 89 (2006);
 A. Djouadi and M. Spira, Phys. Rev. **D62**, 014004 (2000);
 M. Muhlleitner and M. Spira, Nucl. Phys. **B790**, 1 (2008);
 T. Hahn *et al.*, arXiv:hep-ph/0607308 (2006).
137. M. Carena, A. Menon, and C.E.M. Wagner, Phys. Rev. **D76**, 035004 (2007);
 P. Draper, T. Liu, and C.E.M. Wagner, Phys. Rev. **D80**, 035025 (2009).
138. P. Draper, T. Liu, and C.E.M. Wagner, arXiv:0911.0034 [hep-ph].
139. M. Carena *et al.*, Eur. Phys. J. **C45**, 797 (2006).
140. DØ Collab., Phys. Rev. Lett. **101**, 221802 (2008).

141. (***) DØ Collab., DØ Note 5726-CONF, “Search for Neutral Higgs Bosons in Multi- b -jet events in $p\bar{p}$ Collisions at $\sqrt{s} = 1.96$ TeV” (2008).
142. (**) CDF Collab., CDF Note 10105, “Search for Higgs Bosons Produced in Association with b-Quarks” (2010).
143. DØ Collab., Phys. Rev. Lett. **104**, 151801 (2010).
144. CDF Collab., Phys. Rev. Lett. **103**, 201801 (2009).
145. DØ Collab., Phys. Rev. Lett. **101**, 071804 (2008).
146. (***) DØ Collab., DØ Note 5740-CONF, ”Search for MSSM Higgs Boson Production in Di-tau Final States with $\mathcal{L} = 2.2 \text{ fb}^{-1}$ at the DØ Detector” (2008).
147. CDF and D0 Collaborations and the Tevatron New Physics and Higgs Working Group, [arXiv:1003.3363 \[hep-ex\]](https://arxiv.org/abs/1003.3363).
148. S. Gennai *et al.*, Eur. Phys. J. **C52**, 383 (2007).
149. A.D. Sakharov, JETP Lett. **5**, 24 (1967).
150. M. Carena *et al.*, Nucl. Phys. **B599**, 158 (2001).
151. S. Dimopoulos and S. Thomas, Nucl. Phys. **B465**, 23, (1996);
S. Thomas, Int. J. Mod. Phys. **A13**, 2307 (1998).
152. A. Pilaftsis and C.E.M. Wagner, Nucl. Phys. **B553**, 3 (1999).
153. M. Carena *et al.*, Nucl. Phys. **B586**, 92 (2000).
154. A. Pilaftsis, Phys. Rev. **D58**, 096010 (1998); Phys. Lett. **B435**, 88 (1998);
K.S. Babu *et al.*, Phys. Rev. **D59**, 016004 (1999).
155. G.L. Kane and L.-T. Wang, Phys. Lett. **B488**, 383 (2000);
S.Y. Choi, M. Drees, and J.S. Lee, Phys. Lett. **B481**, 57 (2000);
S.Y. Choi and J.S. Lee, Phys. Rev. **D61**, 015003 (2000);
S.Y. Choi, K. Hagiwara, and J.S. Lee, Phys. Rev. **D64**, 032004 (2001); Phys. Lett. **B529**, 212 (2002);
T. Ibrahim and P. Nath, Phys. Rev. **D63**, 035009 (2001);
T. Ibrahim, Phys. Rev. **D64**, 035009 (2001);
S. Heinemeyer, Eur. Phys. J. **C22**, 521 (2001);
S.W. Ham *et al.*, Phys. Rev. **D68**, 055003 (2003).
156. M. Frank *et al.*, JHEP **0702**, 047 (2007);
S. Heinemeyer *et al.*, Phys. Lett. **B652**, 300 (2007);
T. Hahn *et al.*, [arXiv:0710.4891](https://arxiv.org/abs/0710.4891) (2007).
157. D.A. Demir, Phys. Rev. **D60**, 055006 (1999);
S. Y. Choi *et al.*, Phys. Lett. **B481**, 57 (2000).

158. E. Christova *et al.*, Nucl. Phys. **B639**, 263 (2002) [E: Nucl. Phys. **B647**, 359 (2002)].
159. K. E. Williams and G. Weiglein, arXiv:0710.5320 (2007).
160. W. de Boer and C. Sander, Phys. Lett. **B585**, 276 (2004);
 S. Heinemeyer *et al.*, JHEP **0608**, 052 (2006);
 A. Djouadi *et al.*, Phys. Rev. Lett. **78**, 3626 (1997); Phys. Rev. D 57 (1998) 4179;
 S. Heinemeyer and G. Weiglein, JHEP 10 (2002) 072;
 J. Haestier *et al.*, JHEP **0512**, 027, (2005);
 S. Heinemeyer, W. Hollik, and G. Weiglein, Phys. Rept. **425**, 265 (2006);
 S. Heinemeyer *et al.*, arXiv:0710.2972 (2007).
161. O. Buchmueller *et al.*, Eur. Phys. J. **C64**, 391 (2009).
162. O. Buchmueller *et al.*, Phys. Rev. **D81**, 035009 (2010).
163. G. D'Ambrosio *et al.*, Nucl. Phys. **B645**, 155 (2002).
164. J.R. Ellis *et al.*, JHEP **0708**, 083 (2007).
165. E. Lunghi, W. Porod, and O. Vives, Phys. Rev. **D74**, 075003 (2006).
166. M. Carena *et al.*, Phys. Rev. **D74**, 015009 (2006).
167. DØ Collab., Phys. Rev. Lett. **97**, 021802 (2006);
 CDF Collab., Phys. Rev. Lett. **97**, 062003 (2006);
 idem., Phys. Rev. Lett. **97**, 242004 (2006).
168. (**,***) CDF and DØ Collaborations, CDF Note 9787, DØ Note 5928-CONF, “Combination of DØ and CDF Results on $\Delta\Gamma_s$ and the CP-Violating Phase $\beta_s^{J/\psi\phi}$ ”, (2009).
169. DØ Collab., arXiv:1005.2757 [hep-ex] (2010).
170. CDF Collab., Phys. Rev. Lett. **95**, 221805 (2005);
 DØ Collab., Phys. Rev. **D74**, 031107 (2006);
 (**) CDF Collab., CDF Note 9892, “Search for $B_s^0 \rightarrow \mu^+\mu^-$ and $B_d^0 \rightarrow \mu^+\mu^-$ Decays in 3.7 fb^{-1} of $p\bar{p}$ Collisions with CDF II” (2009);
 (***) DØ Collab., DØ Note 5906-CONF, “A new expected upper limit on $B_s \rightarrow \mu^+\mu^-$ using 5 fb^{-1} of Run II data” (2009).
171. J. Foster, K.i. Okumura, and L. Roszkowski, JHEP **0508**, 094 (2005); L. Roszkowski, R. Ruiz de Austri, and R. Trotta, JHEP **0707**, 075 (2007); Phys. Lett. **B641**, 452 (2006).
172. G. Buchalla, A.J. Buras, and M.E. Lautenbacher, Rev. Mod. Phys. **68**, 1125 (1996).

173. A. Dedes and A. Pilaftsis, Phys. Rev. **D67**, 015012 (2003).
174. A.J. Buras *et al.*, Phys. Lett. **B546**, 96 (2002).
175. A.J. Buras *et al.*, Nucl. Phys. **B659**, 2 (2003).
176. K.S. Babu and C.F. Kolda, Phys. Rev. Lett. **84**, 228 (2000).
177. M. Misiak *et al.*, Phys. Rev. Lett. **98**, 022002 (2007), and references therein.
178. Heavy Flavor Averaging Group (HFAG),
<http://www.slac.stanford.edu/xorg/hfag/rare/leppho09/rad11/btosg.pdf>.
179. T. Becher and M. Neubert, Phys. Rev. Lett. **98**, 022003 (2007).
180. I. Adachi *et al.*, [Belle Collab.], arXiv:0809.3834 [hep-ex] (2008).
181. B. Aubert *et al.*, [BABAR Collab.], arXiv:0809.4027 [hep-ex] (2008).
182. G. Isidori and P. Paradisi, Phys. Lett. **B639**, 499 (2006).
183. B. Aubert *et al.*, [BABAR Collab.], Phys. Rev. Lett. **100**, 021801 (2008).
184. I. Adachi *et al.*, arXiv:0910.4301 [hep-ex] (2009).
185. U. Nierste, S. Trine, and S. Westhoff, Phys. Rev. **D78**, 015006 (2008).
186. S. Trine, arXiv:0810.3633 [hep-ph] (2008).
187. M. Carena, A. Menon, and C.E.M. Wagner, Phys. Rev. **D79**, 075025 (2009).
188. J. Ellis *et al.*, Phys. Lett. **B653**, 292 (2007).
189. N. Cabibbo, G. R. Farrar, and L. Maiani, Phys. Lett. **B105**, 155 (1981);
 H. Goldberg, Phys. Rev. Lett. **50**, 1419 (1983);
 J.R. Ellis *et al.*, Nucl. Phys. **B238**, 453 (1984);
 G. Bertone, D. Hooper, and J. Silk, Phys. Reports **405**, 279 (2005).
190. M. Carena, D. Hooper, and A. Vallinotto, Phys. Rev. **D75**, 055010 (2007);
 M. Carena, D. Hooper, and P. Skands, Phys. Rev. Lett. **97**, 051801 (2006).
191. A. Djouadi and Y. Mambrini, JHEP **0612**, 001 (2006).
192. J. Ellis, K.A. Olive, and Y. Santoso, Phys. Rev. **D71**, 095007 (2005).
193. A. Djouadi, M. Spira, and P.M. Zerwas, Z. Phys. **C70**, 675 (1996).

194. ALEPH Collab., Phys. Lett. **B543**, 1 (2002);
 DELPHI Collab., Phys. Lett. **B525**, 17 (2002);
 L3 Collab., Phys. Lett. **B575**, 208 (2003);
 OPAL Collab., Eur. Phys. J. **C7**, 407 (1999).
195. (*) ALEPH, DELPHI, L3 and OPAL Collaborations, The LEP Working Group for Higgs Boson Searches, *Search for Charged Higgs Bosons: Preliminary ...*, LHWG-Note/2001-05.
196. A. G. Akeroyd *et al.*, Eur. Phys. J. **C20**, 51 (2001).
197. DELPHI Collab., Eur. Phys. J. **C34**, 399 (2004).
198. J.A. Coarasa *et al.*, Eur. Phys. J. **C2**, 373 (1998).
199. C.S. Li and T.C. Yuan, Phys. Rev. **D42**, 3088 (1990);
 [E: Phys. Rev. **D47**, 2156 (1993)];
 A. Czarnecki and S. Davidson, Phys. Rev. **D47**, 3063 (1993);
 C.S. Li, Y.-S. Wei, and J.-M. Yang, Phys. Lett. **B285**, 137 (1992).
200. J. Guasch, R.A. Jiménez, and J. Solà, Phys. Lett. **B360**, 47 (1995).
201. M. Carena *et al.*, Nucl. Phys. **B577**, 88 (2000).
202. M. Guchait and S. Moretti, *JHEP* **0201**, 001 (2002).
203. R.M. Barnett, H.E. Haber, and D.E. Soper, Nucl. Phys. **B306**, 697 (1988).
204. F. Olness and W.-K. Tung, Nucl. Phys. **B308**, 813 (1988).
205. F. Borzumati, J.-L. Kneur, and N. Polonsky, Phys. Rev. **D60**, 115011 (1999).
206. A. Belyaev *et al.*, *JHEP* **0206**, 059 (2002).
207. L.G. Jin *et al.*, Eur. Phys. J. **C14**, 91 (2000); Phys. Rev. **D62**, 053008 (2000);
 A. Belyaev *et al.*, Phys. Rev. **D65**, 031701 (2002);
 G. Gao *et al.*, Phys. Rev. **D66**, 015007 (2002).
208. S.-H. Zhu, Phys. Rev. **D67**, 075006 (2005);
 T. Plehn, Phys. Rev. **D67**, 014018 (2003).
209. A.A. Barrientos Bendezú, and B.A. Kniehl, Phys. Rev. **D59**, 015009 (1999); Phys. Rev. **D61**, 015009 (2000);
 Phys. Rev. **D63**, 015009 (2001).
210. A.A. Barrientos Bendezú and B.A. Kniehl, Nucl. Phys. **B568**, 305 (2000).
211. A. Krause *et al.*, Nucl. Phys. **B519**, 85 (1998).
212. O. Brein and W. Hollik, Eur. Phys. J. **C13**, 175 (2000).
213. DØ Collab., Phys. Rev. Lett. **82**, 4975 (1999);
idem, **88**, 151803 (2002);

- CDF Collab., Phys. Rev. **D62**, 012004 (2000);
idem, Phys. Rev. Lett. **79**, 357 (1997).
214. CDF Collab., Phys. Rev. Lett. **96**, 042003 (2006).
215. DØ Collab., Phys. Lett. **B682**, 278 (2009).
216. G.B. Gelmini and M. Roncadelli, Phys. Lett. **B99**, 411 (1981);
R.N. Mohapatra and J.D. Vergados, Phys. Rev. Lett. **47**, 1713 (1981);
V. Barger *et al.*, Phys. Rev. **D26**, 218 (1982).
217. B. Dutta and R.N. Mohapatra, Phys. Rev. **D59**, 015018 (1998);
C. S. Aulakh *et al.*, Phys. Rev. **D58**, 115007 (1998);
C. S. Aulakh, A. Melfo, and G. Senjanovic, Phys. Rev. **D57**, 4174 (1998).
218. DELPHI Collab., Phys. Lett. **B552**, 127 (2003).
219. OPAL Collab., Phys. Lett. **B295**, 347 (1992);
idem, **B526**, 221 (2002).
220. L3 Collab., Phys. Lett. **B576**, 18 (2003).
221. OPAL Collab., Phys. Lett. **B577**, 93 (2003).
222. DØ Collab., Phys. Rev. Lett. **93**, 141801 (2004);
DØ Collab., Phys. Rev. Lett. **101**, 071803 (2008).
223. CDF Collab., Phys. Rev. Lett. **93**, 221802 (2004);
CDF Collab., Phys. Rev. Lett. **101**, 121801 (2008).
224. CDF Collab., Phys. Rev. Lett. **95**, 071801 (2005).
225. H.E. Haber, *Proceedings of the 1990 Theoretical Advanced Study Institute in Elementary Particle Physics*, eds. M. Cvetič and Paul Langacker (World Scientific, Singapore, 1991) pp. 340–475, and references therein.
226. S. Glashow and S. Weinberg, Phys. Rev. **D15**, 1958 (1977).
227. P. Fayet, Phys. Lett. **B90**, 104 (1975);
H.-P. Nilles, M. Srednicki, and D. Wyler, Phys. Lett. **B120**, 346 (1983);
J.-M. Frere, D.R.T. Jones, and S. Raby, Nucl. Phys. **B222**, 11 (1983);
J.-P. Derendinger and C.A. Savoy, Nucl. Phys. **B237**, 307 (1984);
B.R. Greene and P.J. Miron, Phys. Lett. **B168**, 226 (1986);
J. Ellis *et al.*, Phys. Lett. **B176**, 403 (1986);
L. Durand and J.L. Lopez, Phys. Lett. **B217**, 463 (1989);
M. Drees, Int. J. Mod. Phys. **A4**, 3635 (1989);
U. Ellwanger, Phys. Lett. **B303**, 271 (1993);

- U. Ellwanger, M. Rausch de Taubenberg, and C.A. Savoy, Phys. Lett. **B315**, 331 (1993); Z. Phys. **C67**, 665 (1995); Phys. Lett. **B492**, 21 (1997);
 P.N. Pandita, Phys. Lett. **B318**, 338 (1993); Z. Phys. **C59**, 575 (1993);
 T. Elliott, S.F. King, and P.L. White, Phys. Lett. **B305**, 71 (1993); Phys. Lett. **B314**, 56 (1993); Phys. Rev. **D49**, 2435 (1994); Phys. Lett. **B351**, 213 (1995);
 K.S. Babu and S.M. Barr, Phys. Rev. **D49**, R2156 (1994);
 S.F. King and P.L. White, Phys. Rev. **D52**, 4183 (1995);
 N. Haba, M. Matsuda, and M. Tanimoto, Phys. Rev. **D54**, 6928 (1996);
 F. Franke and H. Fraas, Int. J. Mod. Phys. **A12**, 479 (1997);
 S.W. Ham, S.K. Oh, and H.S. Song, Phys. Rev. **D61**, 055010 (2000);
 D.A. Demir, E. Ma, and U. Sarkar, J. Phys. **G26**, L117 (2000);
 R. B. Nevezorov and M. A. Trusov, Phys. Atom. Nucl. **64**, 1299 (2001);
 U. Ellwanger and C. Hugonie, Eur. Phys. J. **C25**, 297 (2002);
 U. Ellwanger *et al.*, arXiv:hep-ph/0305109 (2003);
 D. J. Miller and S. Moretti, arXiv:hep-ph/0403137 (2004).
 228. A. Dedes *et al.*, Phys. Rev. **D63**, 055009 (2001);
 A. Menon, D. Morrissey, and C.E.M. Wagner, Phys. Rev. **D70**, 035005, (2004).
 229. R. Dermisek and J. F. Gunion, Phys. Rev. **D76**, 095006 (2007);
 R. Dermisek and J. F. Gunion, Phys. Rev. **D81**, 075003 (2010).
 230. J. R. Espinosa and M. Quiros, Phys. Lett. **B279**, 92 (1992).
 231. U. Ellwanger and C. Hugonie, Mod. Phys. Lett. **A22**, 1581 (2007).
 232. (*) DELPHI Collab., *Interpretation of the searches for Higgs bosons in the MSSM with an additional scalar singlet*, DELPHI 1999-97 CONF 284.
 233. DØ Collab., Phys. Rev. Lett. **103**, 061801 (2009).
 234. P. Batra *et al.*, JHEP **0402**, 043 (2004);
 P. Batra *et al.*, JHEP **0406**, 032 (2004).
 235. M. Dine, N. Seiberg, and S. Thomas, Phys. Rev. **D76**, 095004 (2007) and references therein.

236. J. R. Espinosa and M. Quiros, Phys. Rev. Lett. **81**, 516 (1998).
237. M. Dine, N. Seiberg, and S. Thomas, Phys. Rev. **D76**, 095004 (2007).
238. P. Batra and E. Ponton, Phys. Rev. **D79**, 035001 (2009).
239. M. Carena *et al.*, Phys. Rev. **D81**, 015001 (2010).
240. I. Antoniadis *et al.*, Nucl. Phys. **B831**, 133 (2010).
241. M. Perelstein, Prog. Part. Nucl. Phys. **58**, 247 (2007).
242. M. Schmaltz and D. Tucker-Smith, Ann. Rev. Nucl. Part. Sci. **55**, 229 (2005).
243. C. R. Chen, K. Tobe, and C. P. Yuan, Phys. Lett. **B640**, 263 (2006).
244. G. F. Giudice *et al.*, JHEP **0706**, 045 (2007).
245. J. Hubisz *et al.*, JHEP **0601**, 135 (2006).
246. I. Low, W. Skiba, and D. Smith, Phys. Rev. **D66**, 072001 (2002).
247. G. F. Giudice, R. Rattazzi, and J. D. Wells, Nucl. Phys. **B595**, 250 (2001);
 M. Chaichian *et al.*, Phys. Lett. **B524**, 161 (2002);
 D. Dominici *et al.*, Acta Phys. Polon. **B33**, 2507 (2002);
 J. L. Hewett and T. G. Rizzo, JHEP **0308**, 028 (2003).
248. OPAL Collab., Phys. Lett. **B609**, 20 (2005).
249. S. Chivukula *et al.*, *Dynamical Electroweak Symmetry Breaking*, in this volume.
250. Y. Chikashige *et al.*, Phys. Lett. **B98**, 265 (1981);
 A.S. Joshipura and S.D. Rindani, Phys. Rev. Lett. **69**, 3269 (1992);
 F. de Campos *et al.*, Phys. Rev. **D55**, 1316 (1997).
251. DELPHI Collab., Eur. Phys. J. **C32**, 475 (2004);
 L3 Collab., Phys. Lett. **B609**, 35 (2005);
 OPAL Collab., Phys. Lett. **B377**, 273 (1996).
252. (*) ALEPH, DELPHI, L3 and OPAL Collaborations, The LEP Working Group for Higgs Boson Searches, *Search for Invisible Higgs Bosons: Preliminary ...*, LHWG-Note/2001-06.
253. M. J. Strassler and K. M. Zureck, Phys. Lett. **B651**, 374 (2007).
254. DØ Collab., Phys. Rev. Lett. **103**, 071801 (2009).
255. E.L. Berger *et al.*, Phys. Rev. **D66**, 095001 (2002).
256. W. Loinaz and J. Wells, Phys. Lett. **B445**, 178 (1998);
 X. Calmet and H. Fritzsch, Phys. Lett. **B496**, 190 (2000).

257. ALEPH Collab., Phys. Lett. **B544**, 25 (2002);
 DELPHI Collab., Eur. Phys. J. **C44**, 147 (2005);
 L3 Collab., Phys. Lett. **B583**, 14 (2004);
 OPAL Collab., Eur. Phys. J. **C18**, 425 (2001).
258. (*) The LEP Working Group for Higgs Boson Searches, *Flavour Independent Search for Hadronically Decaying Neutral Higgs Bosons at LEP*, LHWG Note 2001-07.
259. OPAL Collab., Eur. Phys. J. **C18**, 425 (2001);
 DELPHI Collab., Eur. Phys. J. **C38**, 1 (2004).
260. J. Ellis *et al.*, Nucl. Phys. **B106**, 292 (1976);
 A. Abbasabadi *et al.*, Phys. Rev. **D52**, 3919 (1995);
 R.N. Cahn *et al.*, Phys. Lett. **B82**, 113 (1997).
261. G. Gamberini *et al.*, Nucl. Phys. **B292**, 237 (1987);
 R. Bates *et al.*, Phys. Rev. **D34**, 172 (1986);
 K. Hagiwara *et al.*, Phys. Lett. **B318**, 155 (1993);
 O.J.P. Éboli *et al.*, Phys. Lett. **B434**, 340 (1998).
262. A. G. Akeroyd, Phys. Lett. **B368**, 89 (1996);
 H. Haber *et al.*, Nucl. Phys. **B161**, 493 (1979).
263. ALEPH Collab., Phys. Lett. **B544**, 16 (2002);
 DELPHI Collab., Eur. Phys. J. **C35**, 313 (2004);
 OPAL Collab., Phys. Lett. **B544**, 44 (2002).
264. L3 Collab., Phys. Lett. **B534**, 28 (2002).
265. (*) ALEPH, DELPHI, L3, and OPAL Collabs., The LEP Working Group for Higgs Boson Searches, *Search for Higgs Bosons Decaying into Photons: Combined ...*, LHWG Note/2002-02.
266. DØ Collab., Phys. Rev. Lett. **82**, 2244 (1999);
 CDF Collab., Phys. Rev. **D64**, 092002 (2001).
267. DØ Collab., Phys. Rev. Lett. **102**, 231801 (2009);
 CDF Collab., Phys. Rev. Lett. **103**, 061803 (2009).
268. (**) CDF Collab., “Search for a SM Higgs Boson with the Diphoton Final State at CDF,” CDF Note 10065 (2010).
269. (***) DØ Collab., DØ Note 5067-CONF, “Search for Fermiophobic Higgs Boson in $3\gamma + X$ Events” (2007).
270. ALEPH Collab., Eur. Phys. J. **C49**, 439 (2007).
271. G.J. Gounaris *et al.*, Phys. Lett. **B83**, 191 (1979);
 V. Barger *et al.*, Phys. Rev. **D38**, 2766 (1988);
 F. Boudjema and E. Chopin, Z. Phys. **C37**, 85 (1996);
 A. Djouadi *et al.*, Eur. Phys. J. **C10**, 27 (1999).